Review

Not peer-reviewed version

A Comprehensive Survey on Annotation to Clinical Application: Artificial Intelligence for Intracranial Hemorrhage Detection and Segmentation in Neuroimaging

Mehdi Hosseini Chagahi , Ali Gohari Nezhad , Aein Bahadori , Mohammad Jafari Vayeghan , Saeed Mohammadi Dashtaki , Aramesh M. , Amin Zarei Manoujan , Alireza Samari , Mostafa Omrani , Amin Ghahramani , Behzad Moshiri * , Md. Jalil Piran *

Posted Date: 30 July 2025

doi: 10.20944/preprints202507.2393.v1

Keywords: intracranial hemorrhage; artificial intelligence; medical image analysis; brain hemorrhage segmentation; ICH classification; image fusion; explainable AI

 doi:10.20944/preprints202507.2393.v1

Review

A Comprehensive Survey on Annotation to Clinical Application: Artificial Intelligence for Intracranial Hemorrhage Detection and Segmentation in Neuroimaging

Mehdi Hosseini Chagahi [1], Ali Gohari Nezhad [2], Aein Bahadori [3], Mohammad Jafari Vayeghan [1], Saeed Mohammadi Dashtaki [1], Aramesh M. [4], Amin Zarei Manoujan [4], Alireza Samari [4], Mostafa Omrani [5], Amin Ghahramani [1], Behzad Moshiri [1,6,*] and Md. Jalil Piran [7,*]

[1] Department of Electrical and Computer Engineering, University of Tehran, Tehran 1417614411, Iran
[2] Institute of Petroleum Engineering, School of Chemical Engineering, College of Engineering, University of Tehran, Tehran, Iran
[3] Department of information engineering university of padova, padova, italy
[4] School of Mechanical Engineering, University of Tehran, Tehran, Iran
[5] School of Mechanical Engineering, K. N. Toosi University of Technology, Tehran, Iran
[6] Department of Electrical and Computer Engineering University of Waterloo, Waterloo, Canada
[7] Department of Computer Science and Engineering, Sejong University, Seoul 05006, South Korea
* Correspondence: moshiri@ut.ac.ir (B.M.); piran@sejong.ac.kr (M.J.P.)

Abstract

While artificial intelligence (AI) makes remarkable strides in automating intracranial hemorrhage (ICH) detection, current surveys often focus on narrow aspects of the problem, leaving critical areas such as data labeling, model interpretability, scan-level image fusion, and AI's comparative performance with radiologists inadequately explored. Additionally, challenges like dataset inconsistency, limited generalization across diverse clinical environments, and integration into real-world workflows remain largely unaddressed, hindering the widespread clinical adoption of AI models for ICH detection. This survey aims to fill these gaps by offering a comprehensive, all-encompassing exploration of AI's role in ICH detection. We provide an in-depth analysis that spans the entire diagnostic pipeline, from data annotation, preprocessing, and augmentation to model optimization, complexity reduction, and explainable AI (XAI). In addition, we critically assess AI's performance relative to human radiologists, exploring how AI can augment clinical decision-making rather than replace it. Highlighting advanced scan-level fusion methods like multiple-instance learning and fuzzy decision-making, we present a robust approach for ensuring accurate, reliable, and clinically deployable systems. Through a synthesis of the high-quality studies, this survey not only benchmarks the latest advancements but also identifies key research challenges and future directions necessary to accelerate the clinical integration of AI in ICH detection.

Keywords: intracranial hemorrhage; artificial intelligence; medical image analysis; brain hemorrhage segmentation; ICH classification; image fusion; explainable AI

1. Introduction

1.1. Background

Intracranial hemorrhage (ICH) refers to bleeding that occurs within the skull and is considered one of the most critical and life-threatening neurological emergencies. This condition can arise from a range of causes, including traumatic injuries, aneurysm rupture, high blood pressure, blood clotting disorders, and complications from spinal surgery [1], as well as genetic and hematological conditions [2,3]. Although postoperative ICH is rare, it can manifest within 48 hours after spinal interventions

 doi:10.20944/preprints202507.2393.v1

[4]. In patients with hemophilia, especially children, ICH poses a severe risk with high morbidity and mortality rates [5]. Furthermore, in individuals with hematological disorders or cancer, hemorrhagic events may result from coagulopathy or the presence of intracranial tumors, making ICH a complex and multifactorial condition [6].

While ICH accounts for a relatively small fraction (10–15%) of all strokes, it has a disproportionately high rate of mortality and long-term disability [7]. Alarmingly, about 66% of deaths from neurological disorders are linked to brain hemorrhages, with nearly half occurring within the first 24 hours [8]. Prompt and accurate diagnosis of ICH subtypes, such as intraparenchymal hemorrhage (IPH), intraventricular hemorrhage (IVH), subarachnoid hemorrhage (SAH), chronic or acute subdural hematoma (CSDH/ASDH), and epidural hemorrhage (EDH), is essential for improving clinical outcomes [9].

Neuroimaging, particularly computed tomography (CT), is the most widely used diagnostic modality for detecting ICH due to its speed and availability in emergency settings [10,11]. However, accurate interpretation of CT scans requires significant radiological expertise, and distinguishing between hemorrhage types can be challenging, even for experienced clinicians [12,13]. Factors such as image noise, patient movement, and overlapping visual features can increase the risk of misinterpretation, especially under the time constraints of emergency care [14–17].

Conventional diagnostic systems, including rule-based methods and traditional computer-aided diagnosis (CAD) tools, often lack robustness when confronted with complex or subtle hemorrhages [16,18].

Recent advances in DL, particularly convolutional neural networks (CNNs), attention mechanisms, and transformer-based architectures, proved highly effective in processing medical images, including CT scans of the brain [6,19–23]. These techniques were widely applied in automated ICH detection tasks, and their diagnostic performance showed strong potential for real-world clinical deployment.

For example, Chen et al. in [24] proposed a model that combines depthwise separable convolutions with multi-receptive field mechanisms and Grad-CAM-based visual interpretability. He et al. in [25] introduced a multiscale feature fusion network with attention modules and lesion localization using VGG16 as the core architecture. Ragab et al. in [26] utilized a political optimizer with Faster SqueezeNet and a denoising autoencoder for effective feature extraction and classification. In another hybrid framework, Negm et al. in [27] used a multi-head attention CNN and ensemble classifiers including BiLSTM and stacked autoencoders for ICH detection.

Malik et al. in [28] addressed the issue of uncertain and overlapping features in CT images using a neuro-fuzzy-rough DL model, which achieved notable classification accuracy. Gudadhe et al. in [29] focused on texture-based analysis with ensemble machine learning models to classify hemorrhages using local binary and ternary patterns.

Weakly supervised and multi-task learning approaches were also explored. Zhang et al. in [30] introduced a soft attention model guided by weak segmentation labels to minimize noise interference. Kyung et al. in [31] proposed SMART-Net, a multi-task framework combining classification, segmentation, and reconstruction for more generalized learning. Lee et al. in [32] built an ensemble of pretrained CNNs for explainable and accurate ICH diagnosis from small datasets.

In more recent innovations, Castro et al. in [33] proposed PG-VGPMIL, an advanced multiple-instance learning (MIL) approach using Pólya-Gamma variables for enhanced computational efficiency. Perez et al. in [34] introduced an end-to-end model with CNNs and sparse Gaussian processes trained on scan-level labels for probabilistic classification. Dense-UNet models were adapted for 3D segmentation in traumatic brain injury cases [35], while Sindhura et al. in [36] introduced a unique pipeline using sinogram-based CNN-RNN models to classify ICH without CT reconstruction.

Shah and Jaimin in [37] explored a point-of-care device using machine learning-powered near-infrared spectroscopy to non-invasively detect extravascular brain bleeds. Lin et al. in [38] proposed a semi-supervised learning model to improve generalization by leveraging both labeled and unlabeled

 doi:10.20944/preprints202507.2393.v1

data, achieving superior performance in classification and segmentation tasks. Additionally, Li et al. in [39] developed a novel microwave-induced thermoacoustic tomography (MITAT) method, enhanced by a residual attention U-Net for effective transcranial hemorrhage detection.

In light of these diverse and rapidly evolving approaches, a critical survey of current models is essential. The remainder of this paper will systematically examine and compare the most recent and influential studies in this domain to highlight progress, limitations, and future research directions. The lists of acronyms used throughout this paper are presented in Table 1.

Table 1. List of acronyms and their definitions.

Acronym	Meaning
ICH	Intracranial Hemorrhage
DL	Deep Learning
AI	Artificial Intelligence
IL	Image Labeling
HPO	Hyper-Parameter Optimization
IP	Image Preprocessing
IA	Image Augmentation
CR	Complexity Reduction
SLIM	Scan-Level Image Fusion
AICS	AI in Clinical Settings
AIVR	AI Detection VS. Radiologists
SAH	Subarachnoid Hemorrhage
IVH	Intraventricular Hemorrhage
IPH	Intraparenchymal Hemorrhage
EDH	Epidural Hemorrhage
CSDH	Chronic Subdural Hematoma
ASDH	Acute Subdural Hematoma
NLP	Natural Language Processing
GANs	Generative Adversarial Networks
PO	Political Optimizer
WCO	Willow Catkin Optimization

1.2. Review of Related Survey Articles

AI tools utilize DL algorithms to analyze brain images and accurately identify hemorrhagic sites [40]. These algorithms demonstrate high diagnostic accuracy and improved performance compared to human interpretation alone [41]. They assist healthcare professionals in making rapid and accurate assessments, leading to timely interventions and improved patient outcomes.

In recent years, numerous survey papers investigated the application of AI in the detection and analysis of ICH. These studies provided essential insights into diagnostic performance, methodological advances, and the clinical viability of AI-assisted tools. Below is a summary of the key contributions and focus areas of selected prominent survey papers.

Matsoukas et al. in [42] presented a comprehensive systematic review and meta-analysis evaluating AI algorithms designed for detecting ICH and chronic cerebral microbleeds (CMBs) on non-contrast CT and magnetic resonance imaging (MRI) scans. By analyzing 40 studies on ICH and 19 on CMBs, the authors found that AI systems achieved high sensitivity and specificity (over 92%) for both ICH and CMB detection. The study highlights key challenges including the need for large, well-labeled datasets and reducing false positives.

Jorgensen et al. in [43] performed a meta-analysis comparing convolutional neural networks (CNNs) to radiologists in diagnosing ICH from non-contrast CT scans. The results showed comparable performance, with CNNs achieving pooled sensitivity and specificity above 95%. Although retrospective datasets showed encouraging outcomes, the authors stressed the need for external validation on more diverse cohorts to ensure real-world applicability.

Champawat et al. in [44] offered an extensive literature review spanning 15 years, focusing on the detection and classification of ICH subtypes using CT imaging. The study surveyed various machine learning (ML) and computer vision methods, discussed preprocessing strategies and classification

 doi:10.20944/preprints202507.2393.v1

frameworks, and identified key challenges including dataset limitations, algorithm generalizability, and lack of standardized evaluation metrics.

Maghami et al. in [45] conducted a systematic review and meta-analysis to assess the diagnostic test accuracy of ML algorithms for ICH detection using CT scans. Their study, incorporating both retrospective and prospective works, demonstrated strong diagnostic performance (pooled sensitivity of 91.7% and specificity of 94.5%). Among various architectures, ResNet-based models were highlighted for their superior specificity. The authors emphasized the clinical promise of AI systems, while also calling for further prospective validation.

Ahmed and Prakasam in [12] provided a broad review encompassing both aneurysm and hemorrhage detection via ML techniques. Their work integrated clinical perspectives with technical advancements, highlighting the burden of stroke in low- and middle-income countries and advocating for early detection solutions. The review also addressed issues in diagnosis, hemodynamic modeling, and suggested future research directions that combine imaging with clinical and physiological markers.

Agarwal et al. in [46] critically reviewed AI models for high-volume, first-line neuroimaging tasks such as CT and MRI scans in emergency settings. Uniquely, they limited inclusion to studies that employed external or temporal validation with representative datasets. Their meta-analysis, focused on ICH detection, reported pooled sensitivity and specificity of 90%, and found that many prior studies lacked sufficient methodological rigor. The review strongly argued for higher validation standards and real-world clinical trials.

Hu et al. in [47] conducted a meta-analysis specifically on DL-based detection and segmentation of ICH in acute stroke patients using non-contrast CT. The study included 36 works and found high accuracy (AUC = 0.94, DSC = 0.84), concluding that DL models were comparable to expert clinicians in both detection and segmentation tasks. Furthermore, these models significantly reduced processing time, supporting their potential integration into emergency diagnostic workflows.

While previous survey articles provided valuable overviews of AI applications in ICH detection, most are limited in scope, focusing either solely on classification tasks or a narrow range of DL architectures. Many fail to address the full AI pipeline, including challenges in data annotation, preprocessing variability, explainability, model complexity, and clinical deployment. Furthermore, scan-level decision fusion, critical for aggregating slice-level predictions into reliable scan-level outcomes, was largely overlooked or superficially addressed in earlier reviews. Few papers examine how advanced techniques such as MIL, attention-based fusion, or fuzzy integrals are used to improve scan-level diagnosis. This fragmentation underscores the need for a holistic and clinically relevant synthesis that bridges technical innovation with real-world application. Table 2 compares our survey paper with the latest and best previous reviews.

Table 2. Comparison of our survey with recent related reviews on AI-based ICH detection, highlighting scope, methodology, and clinical focus.

Research	Scope									Contribution
	IL	IP	IA	HPO	SLIF	AIDVR	CR	AICS	XAI	
2022 [43]	✓					✓	✓			CNN vs radiologist performance
2022 [42]	✓			✓				✓		Review of ICH classification approaches; preprocessing overview
2023 [44]	✓		✓	✓			✓	✓		ICH classification review; preprocessing overview
2023 [46]			✓					✓	✓	Focus on validated AI models; Clinical integration
2023 [45]		✓		✓						ML accuracy meta-analysis; ResNet focus
2023 [12]		✓		✓					✓	ICH/aneurysm review; Imaging and hemodynamics
2023 [48]			✓					✓	✓	Validated ICH detection review
2024 [47]	✓	✓					✓	✓		DL model meta-analysis; segmentation speed vs manual
2025 [49]	✓		✓	✓					✓	DL performance synthesis; clinical explainability
Our Survey	✓	✓	✓	✓	✓	✓	✓	✓	✓	Full AI pipeline; Scan-Level Image Fusion Analysis; AI vs. Radiologists; XAI; model deployment

 doi:10.20944/preprints202507.2393.v1

1.3. Contributions of this Survey Article

The main contributions of this survey are summarized as follows.

- The comprehensive AI pipeline covers everything from annotation and preprocessing to model design, optimization, and deployment.
- The study presents an in-depth review of scan-level image fusion (SLIF), including MIL, attention-based, and fuzzy fusion methods for robust scan-level prediction.
- The comparison of AI-based detection and radiologist interpretation highlights their strengths, limitations, and complementary roles.
- The dual focus on tasks provides balanced coverage of ICH detection (classification), segmentation, and localization studies.
- XAI involves the evaluation of Grad-CAM, uncertainty maps, attention mechanisms, and fuzzy logic to enhance clinical interpretability.
- Clinical integration includes a review of FDA-cleared tools, PACS integration, and AI-assisted triage in real-world settings.

1.4. Roadmap of The Survey

This survey provides a comprehensive synthesis of AI-based methods for ICH detection and segmentation in neuroimaging, covering the entire pipeline from annotation to clinical deployment. As illustrated in Figure 1, the structure of the survey is designed to reflect the sequential flow of AI development and application in this domain. The paper begins with an overview of AI in medical imaging and related survey efforts in Section 1, followed by a detailed examination of key components in the AI pipeline in Section 2. These include strategies for image labeling (IL), preprocessing (IP), augmentation (IA), hyperparameter optimization (HPO), complexity reduction (CR), scan-level image fusion (SLIF), explainable AI (XAI), comparison with radiologists (AIDVR), and clinical integration (AICS). In Section 3, we provide a structured synthesis of more than 120 peer-reviewed studies, categorized by task. This includes ICH classification, segmentation, and hybrid/multi-task approaches. Key model architectures, datasets, validation strategies, and performance metrics are analyzed to benchmark the state of the art and assess clinical readiness. Section 4 discusses future research directions, highlighting current limitations and open challenges in standardization, generalizability, and clinical validation. Finally, Section 5 concludes the paper, summarizing key findings and emphasizing the importance of interpretable and clinically integrated AI systems for ICH detection.

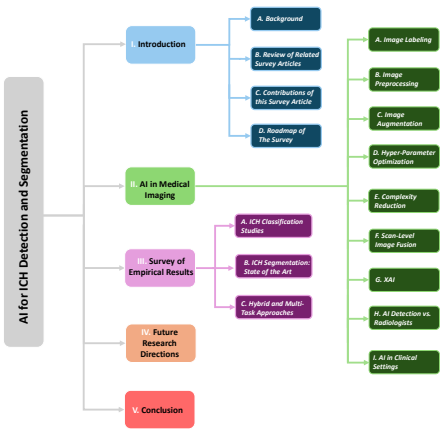

Figure 1. The organizational structure of the survey.

2. AI in Medical Imaging: Techniques, Challenges, and Applications

Figure 2 illustrates the ICH detection workflow leveraging CT slices. The pipeline begins with the input of brain CT images, which are analyzed using DL models for feature extraction. These features are then used to classify the presence or absence of ICH. If ICH is detected, the system

 doi:10.20944/preprints202507.2393.v1

further categorizes it into specific subtypes such as IPH, IVH, SAH, CSDH/ASDH, and EDH. This classification is crucial for guiding clinical interventions based on hemorrhage type and severity.

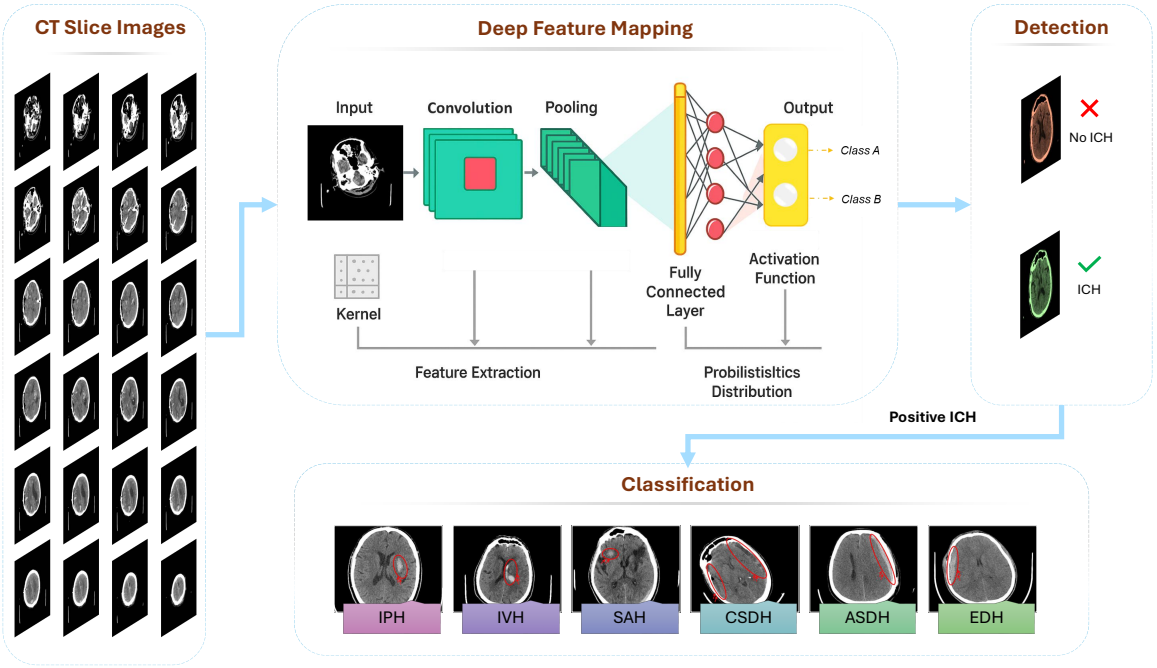

Figure 2. Overview of the ICH Detection pipeline using CT slices: includes image input, deep feature mapping, and hemorrhage subtype classification.

To ensure a comprehensive and systematic review of recent advancements in AI for ICH detection, segmentation, and classification, we conduct a structured literature search across multiple scientific databases. We use a wide range of keyword combinations including, but not limited to: intracranial hemorrhage detection, ICH segmentation, ICH classification, Vision Transformer and ICH, DL and ICH, brain hemorrhage, machine learning, brain hematoma, AI-based ICH, and convolutional neural networks for hemorrhage. These queries are executed across leading academic platforms such as Google Scholar, PubMed, and Scopus to ensure broad coverage of the relevant literature.

The search process is visually summarized in Figure 3. Initially, 375 research articles from the publication window of 2015 to 2025 were identified based on keyword relevance and topic fit. Articles are further filtered based on journal quality (primarily Q1-ranked publications) and citation impact, resulting in a curated set of 127 high-quality studies included in this survey. These articles collectively span the core areas of AI methodologies, clinical integration, explainability, and performance evaluation for ICH diagnosis, forming the foundation of our comprehensive analysis.

 doi:10.20944/preprints202507.2393.v1

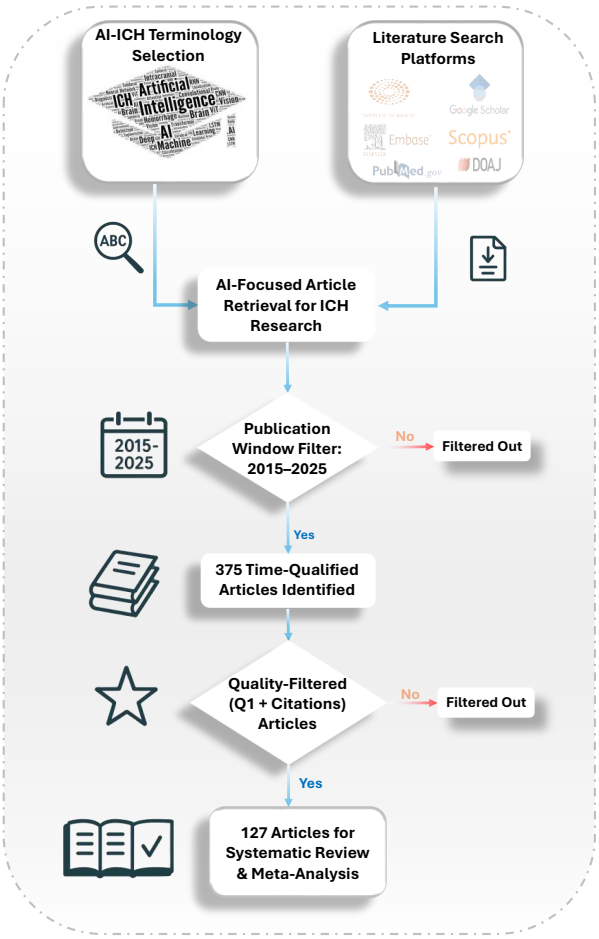

Figure 3. Literature selection workflow: AI-ICH articles are retrieved, filtered by publication date (2015–2025) and quality.

2.1. Image Labeling

A wide range of studies on ICH adopted manual labeling as the primary approach to generate high-quality ground truth data. In these investigations, expert radiologists, sometimes aided by radiology residents, neurosurgeons, or emergency physicians, inspected each CT slice for hemorrhages and then outlined their precise boundaries. Early examples included studies in which radiologists annotated hemorrhage subtypes via a six-digit one-hot vector [50], employed Fujifilm Synapse 3D for meticulous slice-by-slice annotation [51], or converted annotated hemorrhage regions into binary mask images using MATLAB [52]. Other research emphasized the importance of verification by multiple board-certified neuroradiologists, particularly when dealing with subtle hemorrhages [53], as well as the necessity of double-checking all annotations to safeguard against inaccuracies [54–58].

Because manual labeling could be both time-consuming and resource-intensive, several semi-automatic strategies were proposed. Often, these methods leveraged threshold-based or region-growing algorithms to generate an initial segmentation, which was then refined by experts. For instance, researchers used OsiriX to segment hemorrhages with an initial thresholding step followed by manual correction [59], or combined U-Net predictions with radiologist input to correct segmentation masks [60]. In some cases, specialized imaging platforms (e.g., IntelliSpace Discovery or VCAST) provided semi-automated tools that radiologists could tune to reduce labeling burden [59,61,62].

Other authors adopted weakly supervised or scan-level labeling to reduce annotation costs. Under weak supervision, radiology reports or high-level scan labels served as training data without any detailed slice-by-slice or pixel-level segmentation [63–65]. One group combined class activation mapping (CAM) with threshold-based lesion segmentation to generate "weak" labels automatically [66], while others relied on external radiology reports or discharge diagnoses to label scans as hemorrhage-positive

 doi:10.20944/preprints202507.2393.v1

or negative [65,67]. Although these weakly supervised approaches sacrificed fine-grained accuracy, they allowed researchers to handle larger datasets and speed up data preparation.

A dual-level or hybrid labeling approach aimed to benefit from both scan-level annotations and detailed slice-level information. One method automatically assigned scan-level labels by mining radiology reports, then had experts refine slice-level or voxel-level regions of interest [68,69]. Semi-supervised learning frameworks, such as mean-teacher models or uncertainty-guided refinement, also merged fully labeled data with unlabeled or partially labeled scans to improve efficiency [69–71]. In these scenarios, the most uncertain or noise-prone pseudo-labels were discarded or re-verified to manage potential errors.

Finally, several studies pursued fully automatic or synthetic labeling in specialized contexts. Simulation-based research employed k-wave MATLAB toolbox to create synthetic hemorrhage data, automatically assigning labels to mimic real-world acoustic or physical properties [55]. Automatic labeling was also sometimes paired with natural language processing (NLP) to extract hemorrhage details from radiology reports [64,72]. Though these methods dramatically reduced human involvement, they often introduced additional challenges in balancing classes and managing potential mislabeling.

- **Our Insights:** Manual annotations remain the gold standard for accuracy but are expensive and time-consuming. Semi-automatic, weakly supervised, and hybrid approaches aim to ease this burden by leveraging computational tools or scan-level information while still preserving acceptable labeling quality. Ultimately, each method carries its own trade-offs in terms of complexity, cost, and accuracy. Future research will likely focus on refining automated techniques, validating them against expert references, and implementing uncertainty-aware strategies to achieve both high efficiency and high fidelity in labeling ICH data. Figure 4 provides a comparative overview of common data labeling strategies used in ICH research.

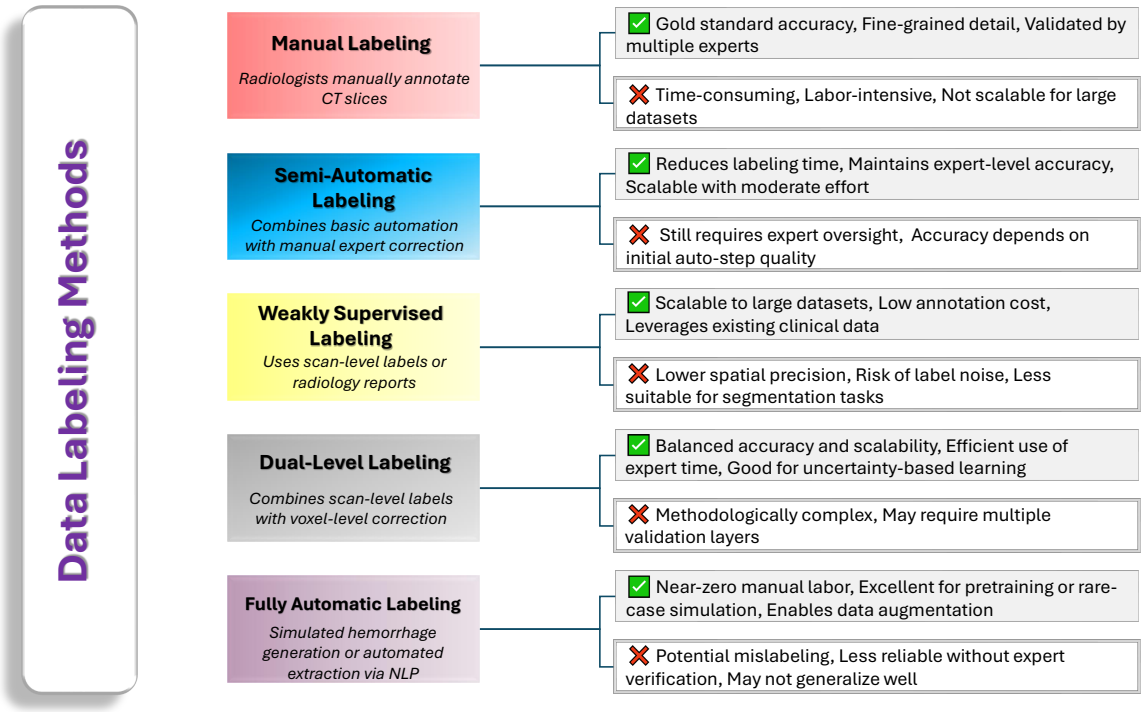

Figure 4. Overview of data labeling methods used in ICH research: manual, semi-automatic, weakly supervised, dual-level, and fully automatic approaches, with their respective trade-offs.

2.2. Image Preprocessing

Various studies utilized a range of techniques aimed at enhancing image quality, removing artifacts, and ensuring consistency across datasets to support DL models.

 doi:10.20944/preprints202507.2393.v1

- Image Windowing and Intensity Adjustments: A common technique employed in multiple studies was the use of windowing, which involved adjusting the contrast of CT images to highlight different tissue types. The brain, bone, and subdural windows were frequently used to emphasize hemorrhage detection and reduce irrelevant background noise. These window settings helped optimize the visibility of critical regions while minimizing false positives in model predictions [50–53]. Windowing was often followed by intensity normalization to standardize the pixel intensity values, ensuring consistency across CT scans from different imaging centers [73–75].
- Noise Reduction and Denoising: Many preprocessing pipelines incorporated denoising techniques, including Gaussian filters, median filters, and morphological operations. These methods helped eliminate noise and small artifacts that could interfere with hemorrhage detection. For example, a study used a 6×6 Gaussian convolution kernel to smooth the segmentation results, while others applied morphological operations like erosion and dilation to refine the boundaries of hemorrhages and remove small unwanted artifacts [66,76,77]. Moreover, bilateral filtering and Gabor filtering were explored in some studies as effective tools for preserving edges while reducing random noise [26,60].
- Skull Stripping and Region Removal: A critical preprocessing step in many studies was skull stripping, which removed the skull and surrounding tissues to focus the model on intracranial structures. This step was particularly important as it reduced irrelevant variations and computational complexity, thereby improving the accuracy of hemorrhage detection. Methods such as thresholding, morphological operations, and the Otsu method were employed to achieve effective skull and background removal [26,53,74,78,79].
- Handling Incomplete or Messy Data: Many studies also emphasized the importance of addressing incomplete or messy data, particularly in clinical settings where some scans may contain motion artifacts, missing slices, or insufficient contrast. Exclusion of scans with these issues or the use of techniques like adaptive thresholding and slice interpolation helped ensure that only high-quality, relevant data was used for training [59,68,72,77]. Some studies also used specialized strategies such as dataset fusion to integrate information across multiple CT slices and correct misclassified hemorrhage regions [73].

- **Our Insights:** The preprocessing of CT scan images plays a crucial role in optimizing the quality of data and enhancing the performance of DL models for ICH detection. Techniques such as image windowing, intensity normalization, noise reduction, skull stripping, and handling incomplete data ensure the accuracy of model predictions by removing artifacts, standardizing input data, and improving the clarity of critical regions. These preprocessing steps are vital for creating consistent and high-quality data, which significantly contributes to the efficiency and reliability of ICH detection models. Figure 5 summarizes different preprocessing techniques are commonly applied to enhance the quality and consistency of CT scan images before they are used for model training.

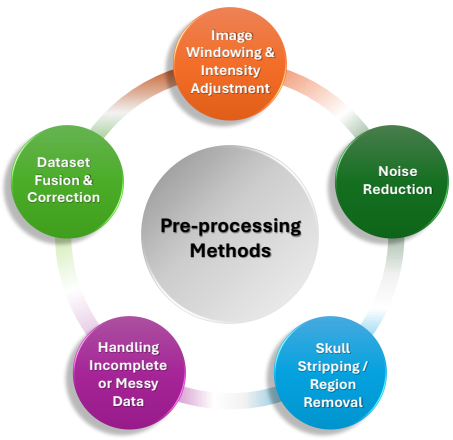

Figure 5. Common preprocessing methods for ICH detection in neuroimaging.

 doi:10.20944/preprints202507.2393.v1

2.3. Image Augmentation

Given the limited availability of labeled medical images, various studies employed numerous augmentation methods to artificially expand the training datasets and enhance model generalization.

Commonly used techniques included geometric transformations such as rotation, flipping, and scaling. These methods aimed to simulate variations in head positioning or imaging orientations, ensuring that the model could detect hemorrhages from different perspectives. For instance, studies applied rotations at various angles, such as 15°, 30°, 45°, or even full rotations (up to 180°), and flipping both horizontally and vertically to create a more diverse range of training images [51,74].

In addition to these, brightness and contrast adjustments, including intensity normalization and scaling, were employed to simulate differences in image acquisition conditions and contrast levels. These techniques helped improve the visibility of hemorrhages and ensure the model's robustness across different imaging modalities and qualities [52,60]. Moreover, random cropping and zooming were used to introduce more variability by altering the region of interest, thus preventing overfitting by forcing the model to focus on various parts of the image [56,80].

Some studies introduced more advanced methods such as non-linear denoising filters, slice interpolation, and synthetic data generation using tools like generative adversarial networks (GANs) to address issues of data scarcity for rare hemorrhage types. By combining these methods with traditional augmentation techniques, models were able to better generalize and perform more accurately on unseen cases [70].

Furthermore, ensemble learning and transfer learning were explored to enhance model performance. Transfer learning, particularly with pre-trained models like ResNet or Inception-ResNet, helped mitigate challenges posed by limited data by leveraging knowledge from other large datasets [17,54,81].

- **Our Insights:** Data augmentation plays a crucial role in overcoming the challenges of limited labeled medical data, particularly in the context of rare hemorrhage subtypes. By employing techniques such as geometric transformations, intensity adjustments, and advanced methods like GANs and transfer learning, researchers can artificially expand training datasets, improve model generalization, and enhance robustness. These strategies help ensure that models are better equipped to detect hemorrhages across varying imaging conditions, orientations, and qualities, thereby addressing data scarcity, class imbalance, and the risk of overfitting. Ultimately, these augmentation techniques are essential for improving the accuracy and reliability of ICH detection models, especially when high-quality annotated data is scarce. Figure 6 summarizes various data augmentation techniques which are often employed alongside labeling strategies.

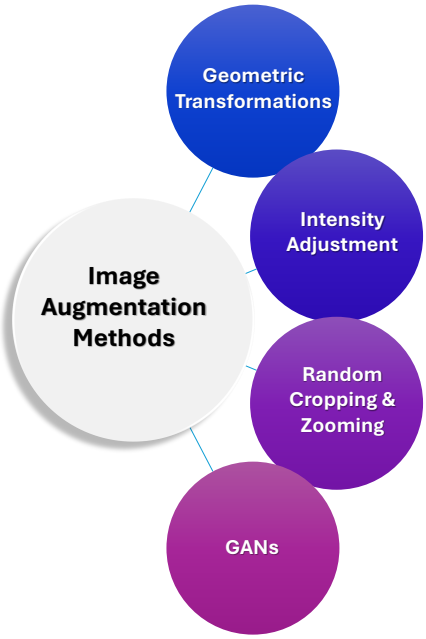

Figure 6. Image augmentation techniques in ICH detection.

 doi:10.20944/preprints202507.2393.v1

2.4. Hyper-Parameter Optimization

Hyperparameter optimization played a critical role in enhancing the performance of ML models, particularly in the challenging task of ICH detection. Different studies adopted various strategies, including both manual and automated methods, to find the most suitable configuration of hyperparameters for DL models.

In many studies, manual optimization was used, where key parameters such as learning rate, batch size, and dropout rate were adjusted through trial and error. For instance, in several studies, researchers manually tuned the learning rate and the number of convolutional blocks or layers to balance model performance and computational efficiency [50,77]. However, manual tuning could be time-consuming and computationally expensive, particularly with complex models like DenseNet201 or when using large datasets [54].

Grid search was a more systematic approach often used for hyperparameter optimization. This technique explored multiple combinations of predefined hyperparameters, selecting the best-performing combination based on validation results. Studies [56,77] utilized grid search to optimize parameters like learning rate, dropout rate, and threshold values for segmentation. While effective, grid search could be computationally intensive as it tested a large number of combinations.

For a more efficient approach, genetic algorithms (GA) and automated learning rate finders were employed. GA allowed for optimization by iterating over multiple generations of hyperparameter sets, selecting the most promising candidates through processes like selection, crossover, and mutation. This technique, used in studies like Jafari and Aein, was particularly useful for optimizing complex hyperparameter spaces, significantly improving model generalizability and reducing errors [26,82].

In more specialized cases, metaheuristic algorithms such as the political optimizer (PO) and willow catkin optimization (WCO) were used to fine-tune models with more complex feature extraction mechanisms. These algorithms dynamically adapted hyperparameters based on real-time feedback, further optimizing model accuracy and reducing the risk of overfitting [26,83]. The use of such advanced techniques enhanced the model's ability to generalize well on unseen data, ensuring better diagnostic performance.

- **Our Insights:** While manual tuning remains a common approach, more advanced methods like grid search, genetic algorithms, and automated learning rate finders have become increasingly popular due to their ability to efficiently explore large hyperparameter spaces. The integration of metaheuristic algorithms further improves model performance by dynamically adapting hyperparameters, ensuring better accuracy and robustness. Figure 7 summarizes the main hyperparameter optimization techniques employed in AI-based ICH detection models.

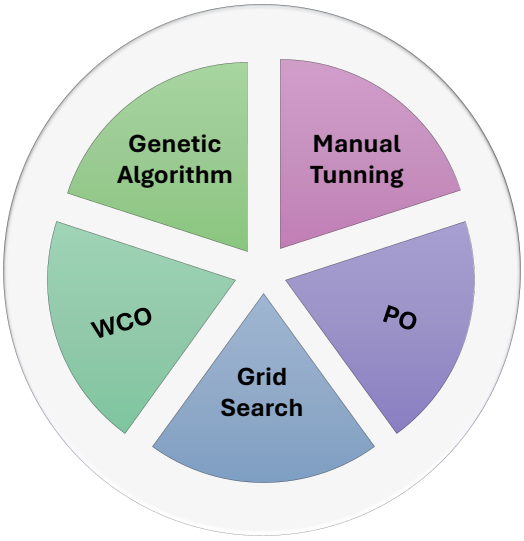

Figure 7. Hyperparameter optimization methods in AI-based ICH detection.

 doi:10.20944/preprints202507.2393.v1

2.5. Complexity Reduction

Complexity reduction was a critical consideration to ensure that models were computationally efficient without compromising diagnostic accuracy. Several strategies were employed across various studies to address this challenge, ensuring that ICH detection models remained suitable for real-time clinical use, especially in resource-constrained environments such as emergency departments.

One widely used approach was the depthwise separable convolution, which reduced the number of parameters and computational load by splitting standard convolutions into smaller, more efficient operations. For instance, studies like [50] demonstrated that by employing depthwise separable convolutions with only 3% of the parameters of MobileNetV3, computational efficiency could be significantly increased without a major drop in model accuracy. This allowed for faster inference times and less resource consumption while retaining diagnostic performance.

In addition, multi-receptive field mechanisms and multi-window conversion strategies were used to compress multiple CT window settings into a single image representation, thereby reducing the number of input channels and the computational demands associated with handling large volumes of data [76]. Moreover, sparse Gaussian processes and attention mechanisms were integrated into models to focus processing power on the most relevant features, thus enhancing efficiency without sacrificing accuracy [84].

Voxel selection procedures and feature selection strategies were other effective ways to manage computational complexity. By selecting only the most informative voxels or features for model training, these methods reduced the dimensionality of the data, which led to faster training times and lower memory usage. Techniques such as feature fusion and dimension reduction also contributed to managing computational resources while maintaining the integrity of important features, as seen in [59,68].

Furthermore, pruning and ghost convolutions were advanced techniques used to reduce model size and computational burden by removing redundant neurons or connections, making the models more efficient without compromising their ability to learn crucial features [74]. These methods allowed the models to run faster and use less memory, which was crucial for deployment in real-time clinical settings.

Several studies also highlighted the effectiveness of transfer learning and automated hyperparameter optimization for complexity reduction. By fine-tuning pre-trained models like ResNet and utilizing optimization algorithms such as GA, models could efficiently adapt to specific tasks without needing to train from scratch, thus saving significant computational resources [26].

Simplified architectures, such as shallow CNNs and reduced versions of U-Net, were introduced to strike a balance between accuracy and complexity. For example, using half U-Net architectures or reducing the number of convolutional channels showed to significantly decrease model complexity while still achieving high segmentation accuracy [26,82].

- **Our Insights:** Techniques such as depthwise separable convolutions, multi-window conversion, voxel and feature selection, pruning, and transfer learning offer effective ways to reduce computational demands without sacrificing diagnostic performance. The ongoing balance between model efficiency and accuracy remains essential, and the use of simpler architectures, optimized for real-time use, continues to be a promising approach for the development of deployable, robust AI models in healthcare settings. Figure 8 summarizes various complexity reduction techniques used in ICH detection models.

 doi:10.20944/preprints202507.2393.v1

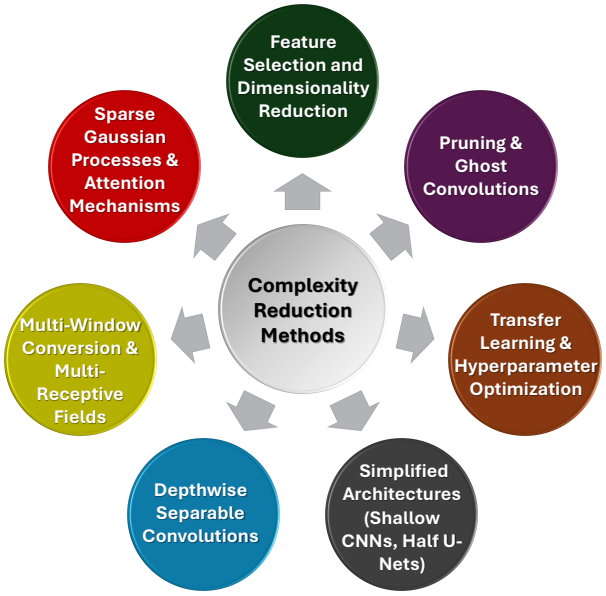

Figure 8. Model complexity reduction techniques in ICH detection.

2.6. Scan-Level Image Fusion

Various studies employed DL techniques to integrate information across multiple CT slices, allowing for a more comprehensive analysis of the brain and more accurate scan-level decisions.

A widely adopted method was MIL, where a CT scan was treated as a "bag" of slices and each slice was an instance without direct labeling. Models using MIL leveraged attention mechanisms to identify the most relevant slices contributing to the overall scan-level classification, thereby learning inter-slice dependencies and focusing on the most informative regions [84]. In addition, cascaded architectures combining CNNs and FCNs were used to segment hemorrhages across slices using dual-window inputs, significantly improving sensitivity and specificity [85].

Ensemble learning strategies also played an important role in scan-level fusion. Methods that aggregated predictions from CNNs, LSTMs, and gradient-boosted trees like XGBoost and CatBoost demonstrated improved classification performance, especially through majority voting and hybrid SVM schemes that ensured robust aggregation across diverse model outputs [86,87].

More recently, a sophisticated technique based on entropy-aware fuzzy integral operators was introduced for scan-level fusion. In this approach, slices were assigned importance weights based on their classification confidence (entropy), and a fuzzy Choquet integral was used to aggregate these confidence scores across all slices. This allowed the model to account for inter-slice dependencies and uncertainty, resulting in more reliable scan-level decisions. For example, the method proposed by Chagahi et al. [88] utilized a pyramid vision transformer (PVT) for feature extraction, followed by SHAP-based feature selection and a fuzzy integral operator to achieve enhanced diagnostic performance in multi-class ICH subtype classification. A similar strategy employing an uncertainty-based fuzzy fusion mechanism was also applied in a co-scale attention model to robustly detect both ICH presence and subdural hemorrhage types from CT scans, further reinforcing the efficacy of fuzzy aggregation in scan-level classification [23].

- **Our Insights:** SLIF is crucial for enhancing the accuracy and efficiency of ICH detection from CT scans by integrating information across multiple slices. Techniques such as MIL, cascaded architectures, and ensemble learning strategies help capture inter-slice dependencies and improve model robustness. Advanced methods like entropy-aware fuzzy integral operators further refine scan-level decisions by considering slice importance and uncertainty, leading to more reliable results. These strategies enable models to focus on the most relevant slices, improve classification performance, and enhance diagnostic accuracy, especially when dealing with complex hemorrhage

 doi:10.20944/preprints202507.2393.v1

types. Overall, scan-level fusion plays a vital role in improving the precision and generalization of ICH detection models. Figure 9 summarizes various image fusion techniques used in ICH detection models.

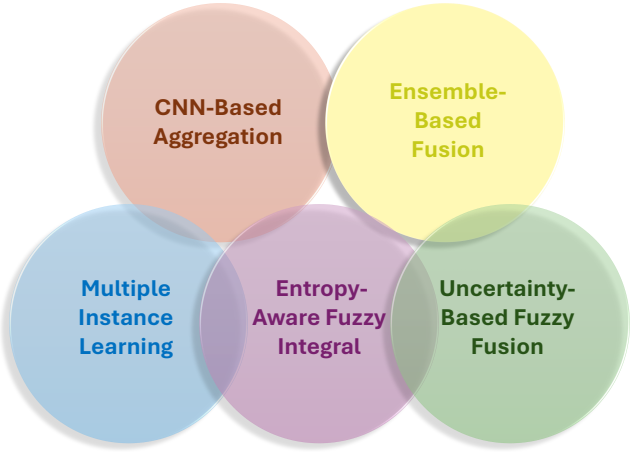

Figure 9. Image Fusion methods for ICH detection in neuroimaging.

2.7. XAI

Several methods were proposed and implemented to improve model transparency, making it easier for clinicians to understand and validate AI-driven predictions.

Gradient-weighted class activation mapping (Grad-CAM) emerged as one of the most widely used techniques for improving model interpretability. This method generated heatmaps that highlighted regions of the input CT scans most influential in the model's decision-making process. Studies [50,70,89] used Grad-CAM to visualize which areas of a scan contributed to a model's classification of hemorrhages. This visual explanation aided clinicians in verifying the model's predictions and fostered trust in its outputs, especially in situations where precise localization of hemorrhage was critical for accurate diagnosis.

Additionally, class activation mapping (CAM), another technique for visualizing model attention, was applied in several studies [78]. CAM helped generate heatmaps that showed high-importance areas, thus enhancing the transparency of the model's decision process and allowing radiologists to detect possible misclassifications. The use of uncertainty maps, as seen in [70,90], provided an additional layer of interpretability by highlighting areas where the model was uncertain. These maps were generated using techniques like Monte Carlo Dropout and entropy-based uncertainty estimation, which helped clinicians identify regions where the model's predictions might require further inspection.

For more advanced interpretability, studies introduced methods like fuzzy inference systems and attention mechanisms. The integration of fuzzy rules in the model, as seen in [71], offered insights into the decision-making process by allowing explicit rule-based reasoning. Attention mechanisms, such as those used in [84,91], focused on highlighting the most relevant slices of a scan, making the model's reasoning clearer and more understandable to clinicians.

Furthermore, logistic regression models and deconvolution techniques were explored as simpler alternatives to DL approaches, offering more straightforward interpretability. The deconvolution technique [77], for instance, helped visualize activations in 3D convolutional networks, providing a reverse mapping of convolutional operations to see which features contributed most to a model's decision.

- **Our Insights:** The integration of explainability techniques into DL models for ICH detection is essential for ensuring trust and clinical acceptance. Techniques like Grad-CAM, CAM, uncertainty maps, and attention mechanisms provide transparency by visualizing the regions of CT scans that influence model decisions, making it easier for clinicians to understand and validate AI

 doi:10.20944/preprints202507.2393.v1

predictions. These methods not only enhance the interpretability of the models but also allow for more informed decision-making, fostering confidence in AI-assisted diagnoses. Furthermore, advanced techniques like fuzzy inference systems and deconvolution offer additional insights into the decision-making process, helping clinicians verify the model's reasoning. Figure 10 summarizes key explainability techniques commonly used in AI-based ICH detection models. While these methods are typically applied during model interpretation, their effectiveness heavily depends on the quality and precision of labeled training data.

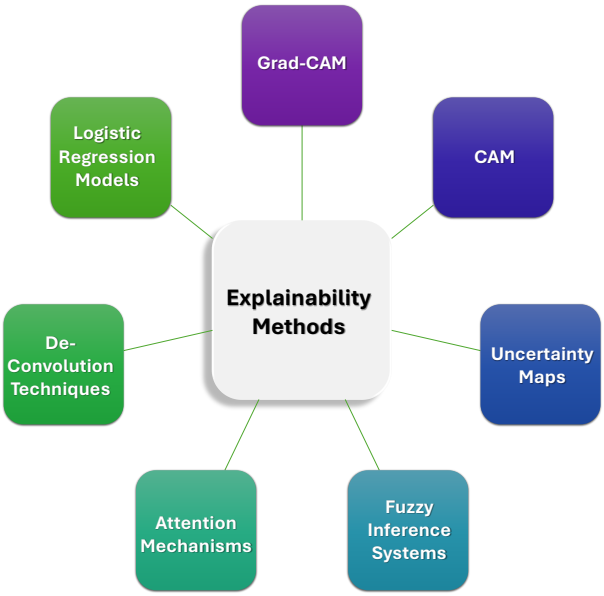

Figure 10. Explainability methods in AI-based ICH detection.

2.8. AI Detection vs. Radiologists Interpretation

Recent studies comparing AI performance with radiologists in detecting ICH showed promising results. In several instances, AI models demonstrated exceptional performance, surpassing radiologists in specific tasks, particularly in detecting subtle hemorrhages or cases with low contrast. For example, the PatchFCN model achieved a high area under the ROC curve (AUC) of 0.991, outperformed several radiologists, and successfully identified subtle hemorrhages that radiologists missed [53]. Moreover, AI systems outperformed junior radiologists in detecting difficult hemorrhage subtypes, such as intraventricular hemorrhages, which were often challenging to detect due to their small size [78].

AI also showed an ability to reduce false-negative rates. In a study, AI-assisted systems reduced radiologists' false-negative rate from 1.6% to near zero in identifying subtle hemorrhages, particularly small subdural bleeds [72]. This highlighted AI's potential as a valuable second-opinion tool, especially in high-pressure environments like emergency rooms. The speed of AI models was another significant advantage, with AI systems processing scans in seconds, compared to several minutes for radiologists, thus reducing workload and speeding up triage [92].

However, AI models still had their limitations. For example, AI systems had a higher tendency to produce false positives, especially in cases where calcifications or vascular structures resembled hemorrhages [72,86]. Additionally, AI models struggled with rare hemorrhage types and scans with artifacts, and their performance heavily depended on the quality and volume of the training data. Radiologists, despite occasional limitations like fatigue or the potential to overlook subtle hemorrhages, brought a level of expertise and adaptability that AI currently could not replicate, especially in ambiguous or noisy cases [74,76].

- **Our Insights:** AI models demonstrated significant potential in improving the accuracy and efficiency of ICH detection, often surpassing radiologists in detecting subtle hemorrhages and reducing false-negative rates. Their ability to process scans rapidly provides a clear advantage in

 doi:10.20944/preprints202507.2393.v1

high-pressure environments, such as emergency rooms, where quick triage is essential. However, AI models are not without limitations, particularly in handling rare hemorrhage types, artifacts, and small lesions. Their performance heavily relies on the quality of training data, and they still tend to produce false positives in certain cases. While AI can be a valuable decision-support tool, it should complement, not replace, radiologists, who bring critical expertise and adaptability to complex or ambiguous cases. Ultimately, the integration of AI as an assistive tool rather than a standalone solution is likely to enhance diagnostic accuracy and efficiency, reducing errors and improving patient outcomes.

2.9. AI in Clinical Settings

Several studies explored AI's role in streamlining radiology workflows and enhancing diagnostic accuracy, with promising results.

AI models, such as those discussed in [76], were implemented to assist radiologists in both retrospective and prospective settings, showcasing high sensitivity and specificity. These systems were designed to provide critical decision support by flagging potential ICH cases, which could then be reviewed by radiologists. In one study, AI was used to analyze CT scans in real-time, acting as a peer reviewer to identify unreported ICH cases, which reduced diagnostic errors significantly. The AI tool was also FDA-cleared, ensuring it met regulatory standards for clinical use, which bolstered its integration into hospital settings [72].

Additionally, AI systems were integrated into existing hospital infrastructures like picture archiving and communication system (PACS), where they could automatically query and retrieve head CT scans and make predictions in real-time. For example, in a prospective implementation, an AI system achieved an accuracy of 96.02% while reducing the time needed to process each scan to approximately 45 seconds [93]. This capability to expedite the diagnostic process was critical in hospitals where delays in reporting could lead to worsened patient outcomes.

In another study, RAPID ICH was deployed as part of a mobile triage platform, processing non-contrast CT (NCCT) studies in under 3 minutes, which significantly expedited the diagnosis of ICH [94]. Similarly, AI tools were used to optimize hospital workflows by upgrading routine CT studies to urgent (stat) status, ensuring that high-risk cases were prioritized and reducing time to diagnosis from hours to just minutes [95,96].

While these AI systems demonstrated clear benefits, several challenges remained. Data variability, the need for large annotated datasets, and concerns about model generalizability across different institutions continued to pose significant hurdles for widespread AI adoption [76,82]. Furthermore, integration with existing hospital workflows could be complex, requiring seamless communication with systems like PACS, which may not always be straightforward. Additionally, AI models often struggled with false positives, especially in cases where artifacts or benign structures were mistaken for hemorrhages [97]. Trust and workload impact were also concerns, with radiologists sometimes skeptical about the AI's recommendations due to its dependence on high-quality labeled data and its potential to misinterpret edge cases [97].

- **Our Insights:** The integration of AI systems into hospital workflows, particularly in emergency settings, showed significant promise in improving the detection and management of ICH. AI proved to be effective in assisting radiologists by enhancing diagnostic accuracy, reducing errors, and streamlining workflows, such as by flagging potential ICH cases and providing real-time analysis. Its ability to process scans quickly, often within seconds, is crucial for timely decision-making in time-sensitive situations. However, challenges such as data variability, the need for large annotated datasets, and integration complexities with existing hospital systems still pose obstacles to widespread adoption. Despite these challenges, AI complements radiologists' expertise by reducing workload, accelerating diagnoses, and improving the accuracy of ICH detection, making it a valuable decision-support tool in busy clinical environments.

 doi:10.20944/preprints202507.2393.v1

3. Review of Empirical Results in AI Applications for ICH Detection

To provide a comprehensive and evidence-driven overview of recent advancements in AI applications for ICH analysis, we present a comparative synthesis of key studies in Tables 3 through 7. These tables compile and categorize more than 60 peer-reviewed research works, covering a broad spectrum of objectives including ICH classification, pixel-level segmentation, and integrated hybrid models that combine both tasks. Each table summarizes critical details such as dataset size, imaging modality, model architecture, validation strategies, and performance metrics, offering a consolidated view of the state of the art.

3.1. ICH Classification Studies

Tables 3 and 4 provide a detailed comparison of the key characteristics and performance outcomes from AI-based classification studies of ICH, organized by public and private datasets, respectively. These tables summarize over 50 studies conducted between 2016 and 2025, incorporating a range of imaging modalities, including CT, NCCT, MRI, and alternative methods such as mNIRS.

Table 3. Summary of public brain imaging datasets and performance metrics used in AI-based ICH Classification studies, including dataset size, modality, model type, validation method, and key results.

Research	Sample	Modality	Objective	Deep Learning Model	Validation	Performance
[98]	N/A	CT	3-Class	CNN + OxfordNet	70/30	AUC = 0.894
[99]	1,940 Slices	MRI	Binary	ResNet18	5-Fold	S_e = 0.91 (Internal), S_e = 0.93 (External)
[58]	613 Slices	MRI	Binary	ResNet34	5-Fold	A_c=1.0
[100]	12635 Scans	CT	Binary	AlexNet-SVM	70/30	A_c =0.934
[101]	42 Scans	MRI	4-Class	AlexNet + VGG16 + ResNet	5-Fold	A_c = 0.952
[102]	372,556 Slices	CT	5-Class	Double-Branch CNN + Random Forest	80/10/10	A_c: 0.951, S_e = 0.867, S_p = 0.917
[103]	82 Slices	CT	5-Class	SVM and FNN	N/A	SVM: A_c=0.806, FNN: A_c=0.867
[86]	27,749 Scans	CT	5-Class	DL model	Train/Test	S_e = 0.913, S_p = 0.941 AUC = 0.954
[97]	27,713 Slices	CT	6-Class	SE-ResNeXt50 + XGBoost, CatBoost, LightGBM	8-Fold	S_e = 0.913, S_p = 0.941 AUC = 0.954
[104]	6,565 Scans	CT	4-Class	Hybrid OzNet	10-Fold	A_c=0.938 ,AUC: 0.993 S_e= 0.939
[96]	750,000 slice	CT	Binary	CNN with Attention	Single-Fold	F_1= 0.839, AUC =0.957
[89]	200 Slices	CT	Binary	ResNet18	80/20	A_c = 0.959, S_e = 0.956, P_r = 0.964, F_1 = 0.959
[66]	752,000 Scans	CT	6-Class	CNN + Attention Network	5-Fold	A_c = 0.981, F_1 = 0.746, AUC = 0.99
[80]	945,920 Slices	CT	6-Class	ResNet34 + Vision Transformer	5-Fold	AUC = 0.983, F_1 = 0.973
[26]	341 Scans	CT	5-Class	Faster SqueezeNet & Denoising Autoencoder	60/40	A_c =0.984, P_r=0.948, R_e=0.908, F_1=0.921
[81]	185,990 Slices	CT	5-Class	SE-ResNeXT + LSTM	k-Fold	A_c = 0.993
[105]	N/A	CT	6-Class	Vision Transformer + MLP	Single-Fold	A_c = 0.893
[71]	573 Scans	NCCT	Binary	Neuro-Fuzzy-Rough Deep Neural Network	5-Fold	A_c = 0.945
[106]	2,501 Slices	CT	Binary	Ensemble Learning Model	90/10	A_c = 0.865
[107]	2,600 Scan	CT	Binary	Hybrid Model: DenseNet121 + LSTM	Train/Val/Test	S_e = 0.959, A_c = 0.975, P_r = 0.970, F_1 = 0.963
[65]	491 Scans	CT	Binary	Attention-Based CNN	K-Fold	AUC = 0.94
[84]	1,640 Scans	CT	Binary	Attention + Gaussian Processes	75/25	A_c = 0.876, F_1 = 0.886, P_r = 0.825
[50]	917,981 Slices	CT	6-Class	CNN+ GRU	5-Fold	AUC = 0.965
[108]	1,310 Scans	CT	6-Class	3D CNN + Bidirectional LSTM	Train/Val/Test	S_e = 0.982, A_c = 0.989, P_r = 0.987, F_1 = 0.984
[109]	874 Scans	NCCT	6-Class	EfficientNetV2 + Transformer Encoder	Train/Val/Test	S_e = 0.976, A_c = 0.983, P_r = 0.975, F_1 = 0.976

 doi:10.20944/preprints202507.2393.v1

Table 4. Summary of private brain imaging datasets and performance metrics used in AI-based ICH Classification studies, including dataset size, modality, model type, validation method, and key results.

Research	Sample	Modality	Objective	Deep Learning Model	Validation	Performance
[110]	46,583 Scans	CT	Binary	Deep CNN	75/5/20	S_e = 0.730, S_p = 0.800 AUC = 0.846
[64]	21,586 Scans	NCCT	6-Class	Qure.ai Algorithms	Train/Test	AUC = 0.92
[111]	1,271 Patients	NCCT	5-Class	3D CNN	5-Fold	F_1 =0.932 ,P_r=0.937, S_e=0.933, S_p=0.987
[112]	15,979 Slices	NCCT	Binary	2D CNN & 3D BiLSTM	Train/Test	A_c: 0.870, S_p= 0.780 S_e= 0.980, AUC = 0.960
[76]	1,300 Scans	CT	6-Class	Ensemble Deep Model	Single-Fold	S_e = 0.920, S_p = 0.950
[87]	110 Patients	CT	Binary	CNN, Aidoc v1.3	80/20	S_e= 0.950, S_p= 0.990, A_c= 0.980
[113]	5,650 Patients	CT	6-Class	Lesion Network	5-Fold	A_c = 0.883
[114]	500 Patients	NCCT	Binary	CNN-MLP	N/A	A_c =0.930, S_e=0.840, S_p=0.940
[115]	200 Scans	CT	Binary	Hybrid (CNN + LSTM, CNN + GRU)	5-Fold	A_c = 0.950
[116]	252 Slices	CT	Binary	Minimalist Machine Learning	N/A	A_c = 0.865, S_p = 0.916
[117]	200 Slices	CT	6-Class	ResNet50	80/10/10	A_c = 0.810, S_e = 0.670, S_p = 0.860
[104]	3,605 Scans	NCCT	Binary	Aidoc (FDA-Cleared AI DSS)	Train/Test	S_e = 0.923, S_p = 0.977
[94]	1,113 Scans	NCCT	Binary	Hybrid 2D-3D CNN	80/20	S_e = 0.956, S_p = 0.953
[118]	2,123 Patients	EMR	Binary	XGBoost	5-Fold	S_e = 0.740, S_p = 0.749 AUC = 0.800
[93]	48,070 Patients	NCCT	6-Class	Joint CNN + RNN with Attention	Train/Test	A_c = 0.994, AUC = 0.998
[119]	134 Patients	CT	Binary	CNNs + Majority Voting	Single-Fold	A_c = 0.626, AUC = 0.660
[83]	341 Scans	CT	5-Class	Majority Voting-Ensemble of RNN and BiLSTM	70/30	A_c =0.984 ,P_r=0.979, S_e=0.928, S_p=0.987
[120]	238 Patients	CT	Binary	SVM	10-Fold	AUC = 0.810
[112]	1,074,271 Slices	CT	5-Class	DenseNet	80/10/10	A_c= 0.949, P_r = 0.854
[26]	341 Scans	CT	5-Class	Faster SqueezeNet + DAE	70/30	A_c = 0.983, P_r = 0.948, S_e = 0.908, F_1 = 0.921
[96]	298 Patients	mNIRS	Binary	DL model	Train/Test	S_e = 0.948, S_p = 0.941, A_c = 0.942
[91]	244 Patients	CT	Binary	CNN+ Vision Transformers	70/30	AUC = 0.930, A_c = 0.840, S_e = 0.790, P_r = 0.950
[23]	31,500 Slices	CT	Binary	Convolutional Attention Network	Single-Fold	A_c=0.984, P_r= 0.980, S_e=0.984, F_1 = 0.981
[88]	36,641 Slices	CT	5-Class	Fuzzy Fusion Network	Single-Fold	A_c=0.963, P_r= 0.949, S_e=0.938, F_1 = 0.943

Table 3 focuses on studies utilizing publicly available datasets like CQ500 and RSNA, which are instrumental in ensuring reproducibility and transparency. These studies span a wide range of dataset sizes, from smaller datasets with fewer than 200 scans to larger public datasets containing hundreds of thousands of slices. These public datasets enable external validation, allowing for greater generalization across diverse clinical environments.

Table 4, on the other hand, highlights studies using private, proprietary datasets that are typically specific to particular institutions. These studies often reflect the application of AI models tailored to the unique imaging conditions, patient demographics, and institutional practices. While these datasets provide more specialized insights, they may lack the generalizability seen in public datasets, making external validation a crucial challenge.

In terms of model architectures, convolutional neural networks CNNs remain dominant, with recent studies exploring more advanced hybrid architectures, such as the integration of recurrent neural networks (e.g., LSTM, GRU), attention mechanisms, and transformers. These approaches aim to better capture the temporal and spatial dependencies inherent in volumetric data, a step toward more sophisticated and nuanced ICH detection systems.

The classification tasks vary from binary decisions (ICH vs. No ICH) to multi-class scenarios involving specific hemorrhage subtypes (e.g., IPH, IVH, SAH, etc.). The shift toward multi-class classification reflects the growing ambition of AI models to address complex diagnostic challenges and provide finer-grained decision support.

Validation strategies in both tables include common methods such as cross-validation (5-fold, 10-fold) and train/validation/test splits. While earlier studies largely relied on internal validation, newer studies emphasize the importance of external validation to ensure the generalizability of AI models in real-world clinical settings.

 doi:10.20944/preprints202507.2393.v1

Performance metrics, including sensitivity (S_e), specificity (S_p), accuracy (A_c), and area under the ROC curve (AUC), show high values across both public and private studies, with many studies reporting AUCs exceeding 0.95. Noteworthy advancements in recent models incorporate fuzzy fusion techniques, attention-based CNNs, and hybrid deep learning approaches, achieving impressive F1-scores (F_1) above 0.95 and accuracy rates approaching or exceeding 0.98, which indicate near-human or superhuman performance in controlled settings.

Despite these advancements, both tables reveal variability in performance, particularly among smaller or earlier studies. This highlights the critical need for standardized evaluation protocols, robust data annotation practices, and large, diverse datasets to ensure the reliability and clinical applicability of AI models for ICH detection.

3.2. ICH Segmentation: State of the Art

Table 5 provides a comprehensive overview of key studies that focus on the segmentation of ICH using brain imaging, particularly CT scans. Segmentation, unlike classification, involves the precise delineation of hemorrhagic regions at the pixel or voxel level, allowing for the quantification of hemorrhage volume and localization of lesion boundaries. This task is critical for clinical decision-making, including surgical planning, monitoring disease progression, and evaluating treatment efficacy.

The studies summarized in Table 5 span a wide range of years, data sources, sample sizes, and DL model architectures. The dataset sizes vary significantly, from relatively small cohorts of fewer than 100 scans to large-scale datasets containing thousands of slices or full-volume scans. Most segmentation studies rely on CT as the imaging modality, reflecting its clinical ubiquity in emergency neuroimaging, although a few investigations also employed magnetic resonance imaging (MRI), especially time-of-flight sequences, in specialized settings.

A notable trend across the timeline of the table is the evolution from classical image processing methods to more advanced DL-based segmentation models. Early methods, such as thresholding and random forests, offered basic binary segmentation with limited precision. As DL techniques matured, architectures like 2D U-Net and 3D CNNs became dominant, offering significant improvements in spatial resolution and segmentation accuracy. More recent advancements introduced attention-based models (e.g., Attention U-Net, SAUNet++, TransUNet), which enhance the network's ability to focus on relevant hemorrhagic regions, even in complex or noisy scans.

Performance metrics reported in Table 5 emphasize the dice similarity coefficient (DSC) as the principal measure of segmentation quality. This metric quantifies the overlap between the predicted segmentation and ground truth annotations. High-performing models often report DSC values above 0.85, with some exceeding 0.90, indicating strong agreement with expert-annotated regions. For example, Dense U-Net and SLEX-Net achieved high Dice scores along with strong accuracy, pixel-wise average precision (AP), and intersection-over-union (IoU) metrics. These results suggest that state-of-the-art models are capable of delivering high-fidelity segmentation outputs that are potentially usable in clinical workflows.

Furthermore, the integration of hybrid models and ensemble techniques also showed promising outcomes. By combining convolutional networks with attention mechanisms, residual connections, or even vision transformers, recent models improved segmentation precision and were more robust to variation in image quality and anatomical complexity. Some models also incorporated auxiliary objectives such as lesion detection or classification, making them suitable for multi-task learning scenarios.

Despite these achievements, several challenges persist. The quality of segmentation is highly dependent on the accuracy of manual annotations, which are labor-intensive and subject to inter-observer variability. Additionally, small and subtle hemorrhages, as well as scans with artifacts or poor contrast, continue to present difficulties for even the most advanced models. These limitations underscore the need for larger, well-annotated datasets and more robust validation strategies.

 doi:10.20944/preprints202507.2393.v1

Table 5. Overview of brain imaging datasets and evaluation results for segmentation-focused ICH studies, highlighting models,validation setups, and segmentation performance(e.g.,Dice score, accuracy).

Research	Dataset	Sample	Modality	Objective	Deep Learning Model	Validation	Performance
[121]	Private	1,800 Slices	3D TOF MRA	Binary	Thresholding Model	90/10	DSC = 0.7, DSC = 0.84
[59]	Public	112 Scans	CT	Binary	Random Forest	Single-Fold	DSI = 0.899
[73]	Private	590 Slices	CT	6-Class	Unsupervised Thresholding-Based Model	Single-Fold	S_e = 0.939, S_p = 1.00, A_c = 0.924, DSC = 0.923
[122]	Private	80 Patients	NCCT	Binary	3D CNN	49/21/30	DSC = 0.910
[123]	Private	66 Patients	TOF, MPRAGE	Binary	U-Net CNN Model	62/16/12	DSC = 0.880
[56]	Public	82 Patients	CT	Binary	U-Net	5-Fold	DSC = 0.310, S_e = 0.972, S_p = 0.504
[124]	Private + Public	25,036 Patients	CT	6-Class	Attention-Based U-Net	5-Fold	DSC = 0.670
[125]	Private	11,000 Slices	NCCT	3-Class	nnU-Net	62/19/19	DSC = 0.806, S_e = 0.873
[126]	Private	3,747 Scans	CT	4-Class	Dense U-Net	80/20	DSC = 0.866
[99]	Private	11,000 Slices	CT	5-Class	SLEX-Net	72/8/20	R^2 = 0.994
[51]	Private	13,658 Slices	CT	3-Class	CNN + FCL	70/30	DSC (Slice-Level) = 0.524 DSC (Patient-Level) = 0.376
[127]	Public	2,814 Slices	CT	5-Class	DenseNet201-U-Net	5-Fold	DSC = 0.857, A_c = 0.990 IoU = 0.843
[128]	Private	2,818 Slices	CT	Binary	DeeplabV3+Res50, SAUNet++, TransUNet	K-Fold	DSC = 0.860, S_e = 0.833, IoU = 0.768, F_1 = 0.849

3.3. Hybrid and Multi-Task Approaches

Tables 6 and 7 provide an in-depth summary of hybrid AI models developed for dual or multi-task processing of ICH in neuroimaging, specifically addressing classification, detection, segmentation, and sometimes localization. These hybrid models are designed to replicate the decision-making processes of expert radiologists by integrating multiple tasks into a single unified framework. The split into public and private studies allows for a focused comparison of models based on dataset accessibility and characteristics.

Table 6. Summary of hybrid AI models for ICH detection and segmentation tasks based on public datasets.

Research	Sample	Modality	Objective	Deep Learning Model	Validation	Performance
[129]	752,000 Slices	CT	Cla + Seg (6-Class)	Weakly-Supervised Guided Soft Attention Network	K-Fold	A_c = 0.981
[130]	1,247 Scans	CT	Det + Seg (Binary)	PatchFCN	75/15/10	Pixel AP= 0.847, Region AP= 0.920, Stack AP= 0.957
[111]	51 Scans	CT	Seg + Det (Binary)	2D U-Net, 3D DenseNet, 3D V-Net	10-Fold	DSC= 0.910
[131]	8,723 Slices	CT	Cla + Seg (Binary)	DL Model	Train/Test	S_e = 0.884, S_p = 0.961
[125]	4,000 Slices	CT	Det + Cla	3D CNN + VGG19	10-Fold	A_c = 0.982, S_e = 0.975, S_p = 0.978, F_1 = 0.999
[132]	147,652 Slices	CT	Seg + Cla	Transfer Learning + LSTM + Conv3D	Single-Fold	AUC = 0.988, F_1 = 0.933, S_e = 0.966, S_p = 0.970, DSC = 0.642
[133]		CT	Det + Cla	CNN-RNN (Cascaded) + U-Net	70/10/20	A_c = 0.955, S_e = 0.931, S_p = 0.971
[134]	372,556 slices	CT	Cla + Det	LGBM	70/30	A_c = 0.977, S_e = 0.965, F_1 = 0.974, P_r = 0.947
[135]	752,799 Slices	NCCT	Det + Cla	EfficientNet + ResNet	90/5/5	A_c = 0.927, AUC = 0.970
[136]	870,301 Slices	CT	Cla + Seg	GA + BiLSTM	5-Fold	S_e = 0.994, A_c = 0.998, S_p = 0.994
[137]	37,872 Slices	CT	Det + Cla	CNN-Based Hybrid Model	Train/Test	S_e = 0.989, A_c = 0.992, S_p = 0.992, F_1 = 0.986
[26]	110 Patients	CT	Cla + Loc (6-Class)	VGG-16 + Attentional Fusion	80/20	AUC = 0.973, AP Score = 0.250
[52]	2,814 Slices	CT	Cla + Seg (6-Class)	Encoder-Decoder Model	10-Fold	S_e = 0.993, P_r = 0.943, F_1 = 0.967, IoU = 0.807, S_p = 0.981, A_c = 0.960
[69]	25,457 Scans	NCCT	Det + Seg (Binary)	PatchFCN + Dilated ResNet38	Train/Test	AUC = 0.939, DSC = 0.829
[138]	491 Patients	CT	Cla + Seg (6-Class)	ResNet, ResNet-SE, HRaNet	80/10/10	AUC = 0.960, Jaccard = 0.913, F_1 = 0.946, Kappa = 0.937
[139]	9,377 Slices	CT	Cla + Loc (5-Class)	YOLO Family	Train/Test	S_e = 0.967, F_1 = 0.970, P_r = 0.979
[140]	2,814 Slices	CT	Cla + Seg (Binary)	ResUNet	5-Fold	S_e = 0.751, A_c = 0.89, Jaccard = 0.441, DSC = 0.613

 doi:10.20944/preprints202507.2393.v1

Table 7. Summary of hybrid AI models for ICH detection and segmentation tasks based on private datasets.

Research	Sample	Modality	Objective	Deep Learning Model	Validation	Performance
[67]	627 Slices	CT	Seg + Cla	Adaboost-DRLSE + SVM	5-Class	Seg: A_c= 0.956 Cla: A_c 0.941
[62]	76,621 Slices	NCCT	Cla + Volume Quantification	ROI-Based CNN	5-Fold	A_c = 0.972, S_e = 0.951, S_p = 0.973
[141]	8,652 Patients	CTA	Seg + Det (Binary)	3D CNN, SE-ResNeXt	75/10/15	S_e = 0.890, S_p = 0.975, A_c = 0.932
[142]	135,497 Slices	CT	Cla + Seg (5-Class)	GoogleNet + Dual FCN	5-Fold	A_c = 0.982
[85]	135,974 Slices	NCCT	Cla + Seg (5-Class)	Dual CNNs	5-Fold	S_e = 0.979, S_p = 0.987, P_r = 0.801, S_e = 0.821
[53]	4,596 Scans	CT	Seg + Cla (6-Class)	FCN + ResNet38	4-Fold	AUC = 0.991
[143]	2,836 Patients	NCCT	Det + Cla	Joint CNN + RNN	80/10/10	A_c = 0.990, S_e = 0.990
[144]	12,000 Slices	NCCT	Det + Cla	3D CNN	5-Fold	S_e = 0.750, P_r = 0.666, F_1 = 0.706
[145]	N/A	CT	Seg + Cla	Capsule Network + Fuzzy DNN	Train/Test	P_r = 0.949, A_c = 0.985
[146]	82 Patients	CT	Cla + Seg (6-Class)	GrabCut + Synergic Deep Learning	Multi-run	A_c = 0.957, P_r = 0.957, S_e = 0.940, S_p = 0.977
[147]	372,556 Slices	CT	Det + Cla	Double-Branch CNN + SVM + RF	80/10/10	A_c = 0.954
[61]	253	CTA	Seg + Det (Binary)	Ensemble Deep Learning	5-Fold	S_e = 0.960, DSC = 0.870
[148]	54 Scans	CT	Det + Seg (Binary)	U-Net	N/A	Fisher = 0.018, MCR= 0.092
[149]	82 Patients	CT	Cla + Seg (6-Class)	InceptionV4 + MLP	10-Fold	S_e = 0.926, S_p = 0.948, P_r = 0.944, A_c = 0.941
[150]	750 Slices	NCCT	Det + Cla	Mask R-CNN + ResNet50	5-Fold	Det: AUC = 0.907, Cla: AUC = 0.956
[57]	814 Patients	NCCT	Det + Cla	DL Model	Train/Test	A_c = 0.956
[151]	300 Slices	CT	Det + Seg (Binary)	DeepMedic	K-Fold	A_c = 0.890, S_e = 0.820, S_p = 0.900
[92]	2,123 Patients	NCCT	Cla + Seg (5-Class)	Dense-UNet	N/A	A_c = 0.912, S_e = 0.903, S_p = 0.948
[152]	30,222 Slices	CT	Det + Cla	Dual-task Vision Transformer	5-Fold	S_e = 1.00, A_c = 0.998, S_p = 1.00, F_1 = 1.00
[153]	200 Scan	NCCT	Cla + Seg (Binary)	ResNet50 as Encoder + Two Decoders	Train/Val/Test	S_e = 0.921, A_c = 0.925, S_p = 0.930, DSC = 0.783

Both tables showcase the versatility of hybrid architectures, which combine classification and segmentation tasks using DL backbones such as CNNs, U-Nets, ResNets, DenseNets, and cutting-edge models like Vision Transformers, Bidirectional LSTMs, and attention mechanisms. The hybrid models aim to capture both spatial and temporal characteristics of hemorrhages, making them more effective in handling the complexities of neuroimaging data.

Earlier hybrid models in both tables integrated conventional ML algorithms such as AdaBoost or SVM with manually crafted features. More recent approaches moved toward DL-based hybrid architectures, which fused high-capacity feature extractors with interpretable classifiers, providing more accurate and clinically relevant results. Models employing dual-branch networks or CNN-RNN hybrids that processed spatial and sequential data in tandem were prominent in these studies. Additionally, some models incorporated fuzzy logic systems for improved interpretability and uncertainty management, enhancing clinical trust.

In terms of performance, hybrid models typically demonstrate high diagnostic accuracy (often exceeding 95%) and strong segmentation performance (DSC above 0.85 in many cases). Notably, models incorporating spatial attention and temporal modeling, such as EfficientNet with Grad-CAM or ensemble CNN-RNN models, show outstanding results in both classification and segmentation tasks. These advancements indicate the benefit of combining spatial focus with dynamic temporal modeling.

Furthermore, many of the models in both tables integrate explainability components like Grad-CAM, SHAP, or entropy-based attention mechanisms, allowing clinicians to visually interpret the decision-making process of AI systems. This interpretability enhances trust in AI predictions, especially when handling challenging cases like low-contrast hemorrhages or scans with artifacts. Attention-based fusion layers and transformer encoders improve the model's focus on hemorrhagic regions, ensuring robustness in noisy or artifact-prone scans.

 doi:10.20944/preprints202507.2393.v1

In conclusion, Tables 6 and 7 reflect the growing momentum of hybrid AI models in ICH detection and segmentation. These models represent a significant step forward in creating clinically deployable systems capable of handling the multifaceted nature of hemorrhagic stroke diagnosis. By integrating multiple tasks into unified frameworks and improving interpretability, these models demonstrate strong potential for advancing clinical practice. Future work should focus on optimizing these hybrid models for real-time use, ensuring robust validation across diverse populations, and integrating them into clinical workflows to enhance patient outcomes.

4. Future Research Directions

Although AI made notable strides in the detection, segmentation, and localization of ICH, several challenges remain that must be addressed to ensure its full clinical integration.

- One of the most pressing needs is the establishment of standardized benchmarks, including widely accepted datasets and evaluation protocols. The current diversity in data sources, performance metrics, and validation strategies makes it difficult to directly compare models or assess generalizability across clinical environments.
- Improving model robustness and generalizability is another critical direction. Many AI models exhibit high accuracy on internal or curated datasets but fail to maintain performance when applied to scans from different institutions or imaging protocols. Approaches such as cross-domain training, external validation, and federated learning offer promising paths toward creating models that are adaptable to diverse real-world settings.
- Advancing scan-level fusion techniques also holds substantial potential. While some studies have introduced methods like MIL and fuzzy integration, the field would benefit from further research into more adaptive and context-aware fusion strategies. These can improve diagnostic accuracy by capturing inter-slice relationships and enhancing the interpretability of scan-level decisions.
- Equally important is the development of efficient and lightweight models suitable for real-time deployment in clinical environments, particularly in resource-constrained settings like emergency rooms or mobile health platforms. Balancing accuracy with computational efficiency will be key to achieving scalable implementation.
- Future work should also explore the integration of multimodal and clinical data to improve the contextual understanding of ICH presentations. Combining CT imaging with electronic health records, lab data, or alternative imaging modalities such as MRI or mNIRS could enhance diagnostic precision, especially in complex or ambiguous cases.
- Explainability remains a major concern in clinical adoption. As DL models become more complex, it is essential to develop transparent systems that clinicians can trust. Techniques such as attention visualization, uncertainty estimation, and rule-based inference systems should be further refined to support clearer decision-making and accountability.
- The high cost and time requirements of manual annotations limit the scalability of current models. Future research should focus on leveraging semi-supervised, weakly supervised, and active learning frameworks to utilize partially labeled or unlabeled data more effectively, thus reducing the dependency on exhaustive expert annotation.
- Finally, to bridge the gap between research and practice, AI models must undergo rigorous real-world validation through prospective, multi-center clinical trials. These trials should assess not only technical performance but also usability, workflow integration, and their actual impact on diagnostic speed, accuracy, and patient outcomes.

In summary, future research should aim for greater standardization, broader validation, more interpretable and efficient models, and stronger integration with clinical workflows, ultimately enabling AI to play a transformative role in ICH diagnosis and management.

 doi:10.20944/preprints202507.2393.v1

5. Conclusions

In this paper, we surveyed the state-of-the-art AI approaches across the entire diagnostic pipeline, including data annotation techniques, image preprocessing and augmentation, model architectures, hyperparameter optimization, explainability methods, complexity reduction, and clinical deployment strategies. Novel methods such as SLIF, weakly supervised learning, and attention-based frameworks showed great promise in improving diagnostic accuracy and interpretability. Furthermore, comparative studies indicated that AI systems were increasingly able to match or even outperform radiologists in specific diagnostic tasks, particularly when supported by well-designed explainability and uncertainty estimation mechanisms. At the same time, several FDA-cleared tools and hospital-based deployments demonstrated that AI began to make tangible contributions to real-world clinical workflows. Despite these achievements, challenges remained. Issues related to generalizability, standardization, data scarcity, and model transparency had to be addressed to enable broader clinical adoption. Our survey identified these gaps and proposed future directions focused on robust model development, scan-level fusion enhancement, multi-modal data integration, and prospective validation through real-world trials. This survey served as a foundational resource for researchers, clinicians, and developers aiming to advance the frontiers of AI in neuroimaging.

References

1. Huang, H.; Zhu, C.; Qin, H.; Deng, L.; Huang, C.; Saifi, C.; Bondar, K.; Giordan, E.; Danisa, O.; Chung, J.H.; et al. Intracranial hemorrhage after spinal surgery: a literature review. *Annals of Translational Medicine* **2022**, *10*.
2. Akyol, Ş.; Koçak Gül, D.; Yılmaz, E.; Karaman, Z.F.; Özcan, A.; Küçük, A.; Gök, V.; Aydın, F.; Per, H.; Karakükcü, M.; et al. Intracranial hemorrhage in children with hemophilia. *Journal of Translational and Practical Medicine* **2022**, pp. 85–88.
3. Feng, X.; Li, X.; Feng, J.; Xia, J. Intracranial hemorrhage management in the multi-omics era. *Heliyon* **2023**.
4. Zhang, J.Y.; Li, Y.; Ma, Y.S.; Sun, X.J.; Liu, Y.Z.; Yin, Y.K.; Hu, B.; Su, M.H.; Li, Q.L.; Mi, Y.C.; et al. Clinical characteristics and prognostic factors in intracranial hemorrhage patients with hematological diseases. *Annals of Hematology* **2022**, *101*, 2617–2625.
5. Rogers, L.R. Intracranial haemorrhage in cancer patients. In *Handbook of Neuro-Oncology Neuroimaging*; Elsevier, 2022; pp. 87–91.
6. Ren, Z.; Liu, S.; Wang, L.; Guo, Z. Conv-SdMLPMixer: A hybrid medical image classification network based on multi-branch CNN and multi-scale multi-dimensional MLP. *Information Fusion* **2025**, p. 102937.
7. Renedo, D.; Acosta, J.N.; Leasure, A.C.; Sharma, R.; Krumholz, H.M.; De Havenon, A.; Alahdab, F.; Aravkin, A.Y.; Aryan, Z.; Barnighausen, T.W.; et al. Burden of ischemic and hemorrhagic stroke across the US from 1990 to 2019. *JAMA neurology* **2024**, *81*, 394–404.
8. Smith, E.R. Cavernous malformations of the central nervous system. *New England Journal of Medicine* **2024**, *390*, 1022–1028.
9. Neethi, A.; Kannath, S.K.; Kumar, A.A.; Mathew, J.; Rajan, J. A comprehensive review and experimental comparison of deep learning methods for automated hemorrhage detection. *Engineering Applications of Artificial Intelligence* **2024**, *133*, 108192.
10. Bhat, N.; Biradar, V.G.; Mallya, A.K.S.; Sabat, S.S.; Pareek, P.K.; et al. Identification of Intracranial Hemorrhage using ResNeXt Model. In Proceedings of the 2022 IEEE 2nd Mysore Sub Section International Conference (MysuruCon). IEEE, 2022, pp. 1–5.
11. Dehghan Rouzi, M.; Moshiri, B.; Khoshnevisan, M.; Akhaee, M.A.; Jaryani, F.; Salehi Nasab, S.; Lee, M. Breast cancer detection with an ensemble of deep learning networks using a consensus-adaptive weighting method. *Journal of Imaging* **2023**, *9*, 247.
12. Ahmed, S.N.; Prakasam, P. A systematic review on intracranial aneurysm and hemorrhage detection using machine learning and deep learning techniques. *Progress in Biophysics and Molecular Biology* **2023**.
13. Bayoudh, K. A survey of multimodal hybrid deep learning for computer vision: Architectures, applications, trends, and challenges. *Information Fusion* **2024**, *105*, 102217.
14. Li, Q.; Yakhkind, A.; Alexandrov, A.W.; Alexandrov, A.V.; Anderson, C.S.; Dowlatshahi, D.; Frontera, J.A.; Hemphill, J.C.; Ganti, L.; Kellner, C.; et al. Code ICH: a call to action. *Stroke* **2024**, *55*, 494–505.

 doi:10.20944/preprints202507.2393.v1

15. Wang, R.; Shi, X.; Pang, S.; Chen, Y.; Zhu, X.; Wang, W.; Cai, J.; Song, D.; Li, K. Cross-attention guided loss-based deep dual-branch fusion network for liver tumor classification. *Information Fusion* **2025**, *114*, 102713.
16. Chagahi, M.H.; Dashtaki, S.M.; Moshiri, B.; Piran, M.J. Cardiovascular disease detection using a novel stack-based ensemble classifier with aggregation layer, DOWA operator, and feature transformation. *Computers in Biology and Medicine* **2024**, *173*, 108345.
17. Chagahi, M.H.; Dashtaki, S.M.; Delfan, N.; Mohammadi, N.; Samari, A.; Moshiri, B.; Piran, M.J.; Acharya, U.R.; Faust, O. Enhancing Osteoporosis Detection: An Explainable Multi-Modal Learning Framework with Feature Fusion and Variable Clustering. *arXiv preprint arXiv:2411.00916* **2024**.
18. Nizarudeen, S.; Shanmughavel, G.R. Comparative analysis of ResNet, ResNet-SE, and attention-based RaNet for hemorrhage classification in CT images using deep learning. *Biomedical Signal Processing and Control* **2024**, *88*, 105672.
19. Delfan, N.; Moghadam, P.K.; Khoshnevisan, M.; Chagahi, M.H.; Hatami, B.; Asgharzadeh, M.; Zali, M.; Moshiri, B.; Moghaddam, A.M.; Khalafi, M.A.; et al. AI-Driven Non-Invasive Detection and Staging of Steatosis in Fatty Liver Disease Using a Novel Cascade Model and Information Fusion Techniques. *arXiv preprint arXiv:2412.04884* **2024**.
20. Iqbal, S.; Qureshi, A.N.; Aurangzeb, K.; Alhussein, M.; Wang, S.; Anwar, M.S.; Khan, F. Hybrid parallel fuzzy CNN paradigm: Unmasking intricacies for accurate brain MRI insights. *IEEE Transactions on Fuzzy Systems* **2024**.
21. Ding, W.; Zhou, T.; Huang, J.; Jiang, S.; Hou, T.; Lin, C.T. FMDNN: A Fuzzy-guided Multi-granular Deep Neural Network for Histopathological Image Classification. *IEEE Transactions on Fuzzy Systems* **2024**.
22. Zhang, L.; Wang, Q.; Zhao, S.; Liu, D.; Li, C.; Wang, B.; Wang, X. Deep-Learning-Based Microwave-Induced Thermoacoustic Tomography Applying Realistic Properties of Ultrasound Transducer. *IEEE Transactions on Microwave Theory and Techniques* **2024**.
23. Chagahi, M.H.; Piran, M.J.; Delfan, N.; Moshiri, B.; Parikhan, J.H. AI-Powered Intracranial Hemorrhage Detection: A Co-Scale Convolutional Attention Model with Uncertainty-Based Fuzzy Integral Operator and Feature Screening. *arXiv preprint arXiv:2412.14869* **2024**.
24. Chen, Y.R.; Chen, C.C.; Kuo, C.F.; Lin, C.H. An efficient deep neural network for automatic classification of acute intracranial hemorrhages in brain CT scans. *Computers in Biology and Medicine* **2024**, *176*, 108587.
25. He, B.; Xu, Z.; Zhou, D.; Zhang, L. Deep multiscale convolutional feature learning for intracranial hemorrhage classification and weakly supervised localization. *Heliyon* **2024**, *10*.
26. Ragab, M.; Salama, R.; Alotaibi, F.S.; Abdushkour, H.A.; Alzahrani, I.R. Political optimizer with deep learning based diagnosis for intracranial hemorrhage detection. *IEEE Access* **2023**, *11*, 71484–71493.
27. Negm, N.; Aldehim, G.; Nafie, F.M.; Marzouk, R.; Assiri, M.; Alsaid, M.I.; Drar, S.; Abdelbagi, S. Intracranial Haemorrhage Diagnosis Using Willow Catkin Optimization With Voting Ensemble Deep Learning on CT Brain Imaging. *IEEE Access* **2023**.
28. Malik, P.; Vidyarthi, A. A Computational Deep Fuzzy Network-Based Neuroimaging Analysis for Brain Hemorrhage Classification. *IEEE Journal of Biomedical and Health Informatics* **2023**.
29. Gudadhe, S.S.; Thakare, A.D.; Oliva, D. Classification of intracranial hemorrhage CT images based on texture analysis using ensemble-based machine learning algorithms: A comparative study. *Biomedical Signal Processing and Control* **2023**, *84*, 104832.
30. Zhang, L.; Miao, W.; Zhu, C.; Wang, Y.; Luo, Y.; Song, R.; Liu, L.; Yang, J. A weakly supervised-guided soft attention network for classification of intracranial hemorrhage. *IEEE Transactions on Cognitive and Developmental Systems* **2022**, *15*, 42–53.
31. Kyung, S.; Shin, K.; Jeong, H.; Kim, K.D.; Park, J.; Cho, K.; Lee, J.H.; Hong, G.; Kim, N. Improved performance and robustness of multi-task representation learning with consistency loss between pretexts for intracranial hemorrhage identification in head CT. *Medical Image Analysis* **2022**, *81*, 102489.
32. Lee, H.; Yune, S.; Mansouri, M.; Kim, M.; Tajmir, S.H.; Guerrier, C.E.; Ebert, S.A.; Pomerantz, S.R.; Romero, J.M.; Kamalian, S.; et al. An explainable deep-learning algorithm for the detection of acute intracranial haemorrhage from small datasets. *Nature biomedical engineering* **2019**, *3*, 173–182.
33. Castro-Macias, F.M.; Morales-Alvarez, P.; Wu, Y.; Molina, R.; Katsaggelos, A.K. Hyperbolic Secant representation of the logistic function: Application to probabilistic Multiple Instance Learning for CT intracranial hemorrhage detection. *Artificial Intelligence* **2024**, *331*, 104115.
34. Perez-Cano, J.; Wu, Y.; Schmidt, A.; Lopez-Perez, M.; Morales-Alvarez, P.; Molina, R.; Katsaggelos, A.K. An end-to-end approach to combine attention feature extraction and Gaussian Process models for deep multiple instance learning in CT hemorrhage detection. *Expert Systems with Applications* **2024**, *240*, 122296.

 doi:10.20944/preprints202507.2393.v1

35. D'Angelo, T.; Bucolo, G.M.; Kamareddine, T.; Yel, I.; Koch, V.; Gruenewald, L.D.; Martin, S.; Alizadeh, L.S.; Mazziotti, S.; Blandino, A.; et al. Accuracy and time efficiency of a novel deep learning algorithm for Intracranial Hemorrhage detection in CT Scans. *La radiologia medica* **2024**, pp. 1–8.
36. Sindhura, C.; Al Fahim, M.; Yalavarthy, P.K.; Gorthi, S. Fully automated sinogram-based deep learning model for detection and classification of intracranial hemorrhage. *Medical Physics* **2024**, *51*, 1944–1956.
37. Shah, J.; Vithalapara, K.; Malik, S.; Lavania, A.; Solanki, S.; Adhvaryu, N.S. Human factor engineering of point-of-care near infrared spectroscopy device for intracranial hemorrhage detection in Traumatic Brain Injury: A multi-center comparative study using a hybrid methodology. *International Journal of Medical Informatics* **2024**, *184*, 105367.
38. Lin, E.; Yuh, E.L. Semi-supervised learning for generalizable intracranial hemorrhage detection and segmentation. *Radiology: Artificial Intelligence* **2024**, *6*, e230077.
39. Li, C.; Xi, Z.; Jin, G.; Jiang, W.; Wang, B.; Cai, X.; Wang, X. Deep-learning-enabled microwave-induced thermoacoustic tomography based on ResAttU-Net for transcranial brain hemorrhage detection. *IEEE Transactions on Biomedical Engineering* **2023**, *70*, 2350–2361.
40. Smorchkova, A.; Khoruzhaya, A.; Kremneva, E.; Petryaikin, A. Machine learning technologies in CT-based diagnostics and classification of intracranial hemorrhages. *Zhurnal voprosy neirokhirurgii imeni NN Burdenko* **2023**, *87*, 85–91.
41. Yun, T.J.; Choi, J.W.; Han, M.; Jung, W.S.; Choi, S.H.; Yoo, R.E.; Hwang, I.P. Deep learning based automatic detection algorithm for acute intracranial haemorrhage: a pivotal randomized clinical trial. *NPJ Digital Medicine* **2023**, *6*, 61.
42. Matsoukas, S.; Scaggiante, J.; Schuldt, B.R.; Smith, C.J.; Chennareddy, S.; Kalagara, R.; Majidi, S.; Bederson, J.B.; Fifi, J.T.; Mocco, J.; et al. Accuracy of artificial intelligence for the detection of intracranial hemorrhage and chronic cerebral microbleeds: A systematic review and pooled analysis. *La radiologia medica* **2022**, *127*, 1106–1123.
43. Jørgensen, M.D.; Antulov, R.; Hess, S.; Lysdahlgaard, S. Convolutional neural network performance compared to radiologists in detecting intracranial hemorrhage from brain computed tomography: a systematic review and meta-analysis. *European Journal of Radiology* **2022**, *146*, 110073.
44. Champawat, Y.S.; Prakash, C.; et al. Literature Review for Automatic Detection and Classification of Intracranial Brain Hemorrhage Using Computed Tomography Scans. *Robotics, Control and Computer Vision* **2023**, pp. 39–65.
45. Maghami, M.; Sattari, S.A.; Tahmasbi, M.; Panahi, P.; Mozafari, J.; Shirbandi, K. Diagnostic test accuracy of machine learning algorithms for the detection intracranial hemorrhage: a systematic review and meta-analysis study. *BioMedical Engineering OnLine* **2023**, *22*, 114.
46. Agrawal, D.; Poonamallee, L.; Joshi, S. Automated detection of intracranial hemorrhage from head CT scans applying deep learning techniques in traumatic brain injuries: A comparative review. *Indian Journal of Neurotrauma* **2023**.
47. Hu, P.; Yan, T.; Xiao, B.; Shu, H.; Sheng, Y.; Wu, Y.; Shu, L.; Lv, S.; Ye, M.; Gong, Y.; et al. Deep learning-assisted detection and segmentation of intracranial hemorrhage in noncontrast computed tomography scans of acute stroke patients: a systematic review and meta-analysis. *International Journal of Surgery* **2024**, *110*, 3839–3847.
48. Agarwal, S.; Wood, D.; Grzeda, M.; Suresh, C.; Din, M.; Cole, J.; Modat, M.; Booth, T.C. Systematic Review of Artificial Intelligence for Abnormality Detection in High-volume Neuroimaging and Subgroup Meta-analysis for Intracranial Hemorrhage Detection. *Clinical Neuroradiology* **2023**, pp. 1–14.
49. Karamian, A.; Seifi, A. Diagnostic Accuracy of Deep Learning for Intracranial Hemorrhage Detection in Non-Contrast Brain CT Scans: A Systematic Review and Meta-Analysis. *Journal of Clinical Medicine* **2025**, *14*, 2377.
50. Chen, Y.R.; Chen, C.C.; Kuo, C.F.; Lin, C.H. An efficient deep neural network for automatic classification of acute intracranial hemorrhages in brain CT scans. *Computers in Biology and Medicine* **2024**, *176*, 108587.
51. Inkeaw, P.; Angkurawaranon, S.; Khumrin, P.; Inmutto, N.; Traisathit, P.; Chaijaruwanich, J.; Angkurawaranon, C.; Chitapanarux, I. Automatic hemorrhage segmentation on head CT scan for traumatic brain injury using 3D deep learning model. *Computers in Biology and Medicine* **2022**, *146*, 105530.
52. Hoang, Q.T.; Pham, X.H.; Trinh, X.T.; Le, A.V.; Bui, M.V.; Bui, T.T. An efficient CNN-based method for intracranial hemorrhage segmentation from computerized tomography imaging. *Journal of Imaging* **2024**, *10*, 77.

 doi:10.20944/preprints202507.2393.v1

53. Kuo, W.; Hane, C.; Mukherjee, P.; Malik, J.; Yuh, E.L. Expert-level detection of acute intracranial hemorrhage on head computed tomography using deep learning. *Proceedings of the National Academy of Sciences* **2019**, *116*, 22737–22745.
54. Khan, M.M.; Chowdhury, M.E.H.; Arefin, A.S.M.S.; Podder, K.K.; Hossain, M.S.A.; Alqahtani, A.; Murugappan, M.; Khandakar, A.; Mushtak, A.; Nahiduzzaman, M. A Deep Learning-Based Automatic Segmentation and 3D Visualization Technique for Intracranial Hemorrhage Detection Using Computed Tomography Images. *Diagnostics* **2023**, *13*. https://doi.org/10.3390/diagnostics13152537.
55. Li, C.; Xi, Z.; Jin, G.; Jiang, W.; Wang, B.; Cai, X.; Wang, X. Deep-Learning-Enabled Microwave-Induced Thermoacoustic Tomography Based on ResAttU-Net for Transcranial Brain Hemorrhage Detection. *IEEE Transactions on Biomedical Engineering* **2023**, *70*, 2350–2361. https://doi.org/10.1109/TBME.2023.3243491.
56. Hssayeni, M.D.; Croock, M.S.; Salman, A.D.; Al-Khafaji, H.F.; Yahya, Z.A.; Ghoraani, B. Intracranial hemorrhage segmentation using a deep convolutional model. *Data* **2020**, *5*, 14.
57. McLouth, J.; Elstrott, S.; Chaibi, Y.; Quenet, S.; Chang, P.D.; Chow, D.S.; Soun, J.E. Validation of a deep learning tool in the detection of intracranial hemorrhage and large vessel occlusion. *Frontiers in Neurology* **2021**, *12*, 656112.
58. Talo, M.; Baloglu, U.B.; Yıldırım, Ö.; Acharya, U.R. Application of deep transfer learning for automated brain abnormality classification using MR images. *Cognitive Systems Research* **2019**, *54*, 176–188.
59. Muschelli, J.; Sweeney, E.M.; Ullman, N.L.; Vespa, P.; Hanley, D.F.; Crainiceanu, C.M. PItcHPERFeCT: primary intracranial hemorrhage probability estimation using random forests on CT. *NeuroImage: Clinical* **2017**, *14*, 379–390.
60. Ozaltin, O.; Coskun, O.; Yeniay, O.; Subasi, A. Classification of brain hemorrhage computed tomography images using OzNet hybrid algorithm. *International Journal of Imaging Systems and Technology* **2023**, *33*, 69–91, [https://onlinelibrary.wiley.com/doi/pdf/10.1002/ima.22806]. https://doi.org/https://doi.org/10.1002/ima.22806.
61. Shahzad, R.; Pennig, L.; Goertz, L.; Thiele, F.; Kabbasch, C.; Schlamann, M.; Krischek, B.; Maintz, D.; Perkuhn, M.; Borggrefe, J. Fully automated detection and segmentation of intracranial aneurysms in subarachnoid hemorrhage on CTA using deep learning. *Scientific Reports* **2020**, *10*, 21799.
62. Chang, P.D.; Kuoy, E.; Grinband, J.; Weinberg, B.D.; Thompson, M.; Homo, R.; Chen, J.; Abcede, H.; Shafie, M.; Sugrue, L.; et al. Hybrid 3D/2D convolutional neural network for hemorrhage evaluation on head CT. *American Journal of Neuroradiology* **2018**, *39*, 1609–1616.
63. López-Pérez, M.; Schmidt, A.; Wu, Y.; Molina, R.; Katsaggelos, A.K. Deep Gaussian processes for multiple instance learning: Application to CT intracranial hemorrhage detection. *Computer Methods and Programs in Biomedicine* **2022**, *219*, 106783. https://doi.org/https://doi.org/10.1016/j.cmpb.2022.106783.
64. Chilamkurthy, S.; Ghosh, R.; Tanamala, S.; Biviji, M.; Campeau, N.G.; Venugopal, V.K.; Mahajan, V.; Rao, P.; Warier, P. Deep learning algorithms for detection of critical findings in head CT scans: a retrospective study. *The Lancet* **2018**, *392*, 2388–2396.
65. Castro-Macías, F.M.; Morales-Álvarez, P.; Wu, Y.; Molina, R.; Katsaggelos, A.K. Hyperbolic Secant representation of the logistic function: Application to probabilistic Multiple Instance Learning for CT intracranial hemorrhage detection. *Artificial Intelligence* **2024**, *331*, 104115.
66. Zhang, L.; Miao, W.; Zhu, C.; Wang, Y.; Luo, Y.; Song, R.; Liu, L.; Yang, J. A weakly supervised-guided soft attention network for classification of intracranial hemorrhage. *IEEE Transactions on Cognitive and Developmental Systems* **2022**, *15*, 42–53.
67. Shahangian, B.; Pourghassem, H. Automatic brain hemorrhage segmentation and classification algorithm based on weighted grayscale histogram feature in a hierarchical classification structure. *Biocybernetics and Biomedical Engineering* **2016**, *36*, 217–232.
68. Patel, A.; van de Leemput, S.; Prokop, M.; Ginneken, B.; Manniesing, R. Image Level Training and Prediction: Intracranial Hemorrhage Identification in 3D Non-Contrast CT. *IEEE Access* **2019**, *PP*, 1–1.
69. Lin, E.; Yuh, E.L. Semi-supervised learning for generalizable intracranial hemorrhage detection and segmentation. *Radiology: Artificial Intelligence* **2024**, *6*, e230077.
70. Emon, S.H.; Tseng, T.L.B.; Pokojovy, M.; Moen, S.; McCaffrey, P.; Walser, E.; Vo, A.; Rahman, M.F. Uncertainty-Guided Semi-Supervised (UGSS) mean teacher framework for brain hemorrhage segmentation and volume quantification. *Biomedical Signal Processing and Control* **2025**, *102*, 107386.
71. Malik, P.; Vidyarthi, A. A computational deep fuzzy network-based neuroimaging analysis for brain hemorrhage classification. *IEEE Journal of Biomedical and Health Informatics* **2023**.

 doi:10.20944/preprints202507.2393.v1

72. Rao, B.; Zohrabian, V.; Cedeno, P.; Saha, A.; Pahade, J.; Davis, M.A. Utility of artificial intelligence tool as a prospective radiology peer reviewer—Detection of unreported intracranial hemorrhage. *Academic radiology* **2021**, *28*, 85–93.
73. Ray, S.; Kumar, V.; Ahuja, C.; Khandelwal, N. Intensity population based unsupervised hemorrhage segmentation from brain CT images. *Expert Systems with Applications* **2018**, *97*, 325–335.
74. Ferdi, A.; Benierbah, S.; Nakib, A.; Ferdi, Y.; Taleb-Ahmed, A. Quadratic Convolution-based YOLOv8 (Q-YOLOv8) for localization of intracranial hemorrhage from head CT images. *Biomedical Signal Processing and Control* **2024**, *96*, 106611. https://doi.org/https://doi.org/10.1016/j.bspc.2024.106611.
75. Maqsood, S.; Damaševičius, R.; Maskeliūnas, R. Hemorrhage Detection Based on 3D CNN Deep Learning Framework and Feature Fusion for Evaluating Retinal Abnormality in Diabetic Patients. *Sensors* **2021**, *21*.
76. Lee, H.; Yune, S.; Mansouri, M.; Kim, M.; Tajmir, S.H.; Guerrier, C.E.; Ebert, S.A.; Pomerantz, S.R.; Romero, J.M.; Kamalian, S.; et al. An explainable deep-learning algorithm for the detection of acute intracranial haemorrhage from small datasets. *Nature biomedical engineering* **2019**, *3*, 173–182.
77. Ker, J.; Singh, S.P.; Bai, Y.; Rao, J.; Lim, T.; Wang, L. Image thresholding improves 3-dimensional convolutional neural network diagnosis of different acute brain hemorrhages on computed tomography scans. *Sensors* **2019**, *19*, 2167.
78. He, B.; Xu, Z.; Zhou, D.; Zhang, L. Deep multiscale convolutional feature learning for intracranial hemorrhage classification and weakly supervised localization. *Heliyon* **2024**, *10*.
79. Ye, H.; Gao, F.; Yin, Y.; Guo, D.; Zhao, P.; Lu, Y.; Wang, X.; Bai, J.; Cao, K.; Song, Q.; et al. Precise diagnosis of intracranial hemorrhage and subtypes using a three-dimensional joint convolutional and recurrent neural network. *European radiology* **2019**, *29*, 6191–6201.
80. Wang, X.; Liu, Z.; Li, J.; Xiong, G. Vision transformer-based classification study of intracranial hemorrhage. In Proceedings of the 2022 3rd International Conference on Computer Vision, Image and Deep Learning & International Conference on Computer Engineering and Applications (CVIDL & ICCEA). IEEE, 2022, pp. 1–8.
81. Umapathy, S.; Murugappan, M.; Bharathi, D.; Thakur, M. Automated computer-aided detection and classification of intracranial hemorrhage using ensemble deep learning techniques. *Diagnostics* **2023**, *13*, 2987.
82. Rajapakse, J.C.; How, C.H.; Chan, Y.H.; Hao, L.C.P.; Padhi, A.; Adrakatti, V.; Khan, I.; Lim, T. Two-stage approach to intracranial hemorrhage segmentation from head CT images. *IEEE Access* **2024**.
83. Negm, N.; Aldehim, G.; Nafie, F.M.; Marzouk, R.; Assiri, M.; Alsaid, M.I.; Drar, S.; Abdelbagi, S. Intracranial haemorrhage diagnosis using willow catkin optimization with voting ensemble deep learning on CT brain imaging. *IEEE Access* **2023**, *11*, 75474–75483.
84. Pérez-Cano, J.; Wu, Y.; Schmidt, A.; López-Pérez, M.; Morales-Álvarez, P.; Molina, R.; Katsaggelos, A.K. An end-to-end approach to combine attention feature extraction and Gaussian Process models for deep multiple instance learning in CT hemorrhage detection. *Expert Systems with Applications* **2024**, *240*, 122296.
85. Cho, J.; Park, K.S.; Karki, M.; Lee, E.; Ko, S.; Kim, J.K.; Lee, D.; Choe, J.; Son, J.; Kim, M.; et al. Improving sensitivity on identification and delineation of intracranial hemorrhage lesion using cascaded deep learning models. *Journal of digital imaging* **2019**, *32*, 450–461.
86. Salehinejad, H.; Kitamura, J.; Ditkofsky, N.; Lin, A.; Bharatha, A.; Suthiphosuwan, S.; Lin, H.M.; Wilson, J.R.; Mamdani, M.; Colak, E. A real-world demonstration of machine learning generalizability in the detection of intracranial hemorrhage on head computerized tomography. *Scientific Reports* **2021**, *11*, 17051.
87. Chao, T.F.; Lip, G.Y.; Lin, Y.J.; Chang, S.L.; Lo, L.W.; Hu, Y.F.; Tuan, T.C.; Liao, J.N.; Chung, F.P.; Chen, T.J.; et al. Major bleeding and intracranial hemorrhage risk prediction in patients with atrial fibrillation: attention to modifiable bleeding risk factors or use of a bleeding risk stratification score? A nationwide cohort study. *International journal of cardiology* **2018**, *254*, 157–161.
88. Chagahi, M.H.; Delfan, N.; Moshiri, B.; Piran, M.J.; Parikhan, J.H. Vision Transformer for Intracranial Hemorrhage Classification in CT Scans Using an Entropy-Aware Fuzzy Integral Strategy for Adaptive Scan-Level Decision Fusion. *arXiv preprint arXiv:2503.08609* **2025**.
89. Altuve, M.; Pérez, A. Intracerebral hemorrhage detection on computed tomography images using a residual neural network. *Physica Medica* **2022**, *99*, 113–119.
90. Rodrigues, M.A.; Samarasekera, N.; Lerpiniere, C.; Humphreys, C.; McCarron, M.O.; White, P.M.; Nicoll, J.A.; Sudlow, C.L.; Cordonnier, C.; Wardlaw, J.M.; et al. The Edinburgh CT and genetic diagnostic criteria for lobar intracerebral haemorrhage associated with cerebral amyloid angiopathy: model development and diagnostic test accuracy study. *The Lancet Neurology* **2018**, *17*, 232–240.

 doi:10.20944/preprints202507.2393.v1

91. Qiao, X.; Lu, C.; Xu, M.; Yang, G.; Chen, W.; Liu, Z. DeepSAP: a novel brain image-based deep learning model for predicting stroke-associated pneumonia from spontaneous intracerebral hemorrhage. *Academic Radiology* **2024**, *31*, 5193–5203.
92. D'Angelo, T.; Bucolo, G.M.; Kamareddine, T.; Yel, I.; Koch, V.; Gruenewald, L.D.; Martin, S.; Alizadeh, L.S.; Mazziotti, S.; Blandino, A.; et al. Accuracy and time efficiency of a novel deep learning algorithm for Intracranial Hemorrhage detection in CT Scans. *La radiologia medica* **2024**, *129*, 1499–1506.
93. Alis, D.; Alis, C.; Yergin, M.; Topel, C.; Asmakutlu, O.; Bagcilar, O.; Senli, Y.D.; Ustundag, A.; Salt, V.; Dogan, S.N.; et al. A joint convolutional-recurrent neural network with an attention mechanism for detecting intracranial hemorrhage on noncontrast head CT. *Scientific Reports* **2022**, *12*, 2084.
94. Heit, J.; Coelho, H.; Lima, F.; Granja, M.; Aghaebrahim, A.; Hanel, R.; Kwok, K.; Haerian, H.; Cereda, C.; Venkatasubramanian, C.; et al. Automated cerebral hemorrhage detection using RAPID. *American Journal of Neuroradiology* **2021**, *42*, 273–278.
95. Arbabshirani, M.R.; Fornwalt, B.K.; Mongelluzzo, G.J.; Suever, J.D.; Geise, B.D.; Patel, A.A.; Moore, G.J. Advanced machine learning in action: identification of intracranial hemorrhage on computed tomography scans of the head with clinical workflow integration. *NPJ digital medicine* **2018**, *1*, 9.
96. Shah, J.; Vithalapara, K.; Malik, S.; Lavania, A.; Solanki, S.; Adhvaryu, N.S. Human factor engineering of point-of-care near infrared spectroscopy device for intracranial hemorrhage detection in Traumatic Brain Injury: A multi-center comparative study using a hybrid methodology. *International Journal of Medical Informatics* **2024**, *184*, 105367.
97. Salehinejad, H.; Kitamura, J.; Ditkofsky, N.; Lin, A.; Bharatha, A.; Suthiphosuwan, S.; Lin, H.M.; Wilson, J.R.; Mamdani, M.; Colak, E. A real-world demonstration of machine learning generalizability in the detection of intracranial hemorrhage on head computerized tomography. *Scientific Reports* **2021**, *11*, 17051.
98. Van Grinsven, M.J.; van Ginneken, B.; Hoyng, C.B.; Theelen, T.; Sánchez, C.I. Fast convolutional neural network training using selective data sampling: Application to hemorrhage detection in color fundus images. *IEEE transactions on medical imaging* **2016**, *35*, 1273–1284.
99. Li, X.; Luo, G.; Wang, W.; Wang, K.; Gao, Y.; Li, S. Hematoma expansion context guided intracranial hemorrhage segmentation and uncertainty estimation. *IEEE Journal of Biomedical and Health Informatics* **2021**, *26*, 1140–1151.
100. Dawud, A.M.; Yurtkan, K.; Oztoprak, H. Application of deep learning in neuroradiology: brain haemorrhage classification using transfer learning. *Computational Intelligence and Neuroscience* **2019**, *2019*, 4629859.
101. Talo, M.; Yildirim, O.; Baloglu, U.B.; Aydin, G.; Acharya, U.R. Convolutional neural networks for multi-class brain disease detection using MRI images. *Computerized Medical Imaging and Graphics* **2019**, *78*, 101673.
102. Sage, A.; Badura, P. Intracranial hemorrhage detection in head CT using double-branch convolutional neural network, support vector machine, and random forest. *Applied Sciences* **2020**, *10*, 7577.
103. Chen, H.; Khan, S.; Kou, B.; Nazir, S.; Liu, W.; Hussain, A. A smart machine learning model for the detection of brain hemorrhage diagnosis based internet of things in smart cities. *Complexity* **2020**, *2020*, 3047869.
104. Voter, A.F.; Meram, E.; Garrett, J.W.; Yu, J.P.J. Diagnostic accuracy and failure mode analysis of a deep learning algorithm for the detection of intracranial hemorrhage. *Journal of the American College of Radiology* **2021**, *18*, 1143–1152.
105. Zhang, G.; Shi, Y.; Zhang, Q.; Lin, H.; Yang, L.; Lan, P. A Nested Vision Transformer in Vision Transformer Framework for Intracranial Hemorrhage. In Proceedings of the 2023 IEEE 6th International Conference on Automation, Electronics and Electrical Engineering (AUTEEE). IEEE, 2023, pp. 480–486.
106. Gudadhe, S.S.; Thakare, A.D.; Oliva, D. Classification of intracranial hemorrhage CT images based on texture analysis using ensemble-based machine learning algorithms: A comparative study. *Biomedical Signal Processing and Control* **2023**, *84*, 104832.
107. Babu, P.P.S.; Brindha, T. Deep Learning Fusion for Intracranial Hemorrhage Classification in Brain CT Imaging. *International Journal of Advanced Computer Science & Applications* **2024**, *15*.
108. Huang, C.C.; Chiang, H.F.; Hsieh, C.C.; Zhu, B.R.; Wu, W.J.; Shaw, J.S. Impact of Dataset Size on 3D CNN Performance in Intracranial Hemorrhage Classification. *Diagnostics* **2025**, *15*, 216.
109. Gong, W.; Luo, Y.; Yang, F.; Zhou, H.; Lin, Z.; Cai, C.; Lin, Y.; Chen, J. ETDformer: an effective transformer block for segmentation of intracranial hemorrhage. *Medical & Biological Engineering & Computing* **2025**, pp. 1–18.
110. Arbabshirani, M.R.; Fornwalt, B.K.; Mongelluzzo, G.J.; Suever, J.D.; Geise, B.D.; Patel, A.A.; Moore, G.J. Advanced machine learning in action: identification of intracranial hemorrhage on computed tomography scans of the head with clinical workflow integration. *NPJ digital medicine* **2018**, *1*, 9.

 doi:10.20944/preprints202507.2393.v1

111. Patel, A.; Schreuder, F.H.; Klijn, C.J.; Prokop, M.; Ginneken, B.v.; Marquering, H.A.; Roos, Y.B.; Baharoglu, M.I.; Meijer, F.J.; Manniesing, R. Intracerebral haemorrhage segmentation in non-contrast CT. *Scientific reports* **2019**, *9*, 17858.
112. Arman, S.E.; Rahman, S.S.; Irtisam, N.; Deowan, S.A.; Islam, M.A.; Sakib, S.; Hasan, M. Intracranial hemorrhage classification from ct scan using deep learning and bayesian optimization. *IEEE Access* **2023**, *11*, 83446–83460.
113. Karki, M.; Cho, J.; Lee, E.; Hahm, M.H.; Yoon, S.Y.; Kim, M.; Ahn, J.Y.; Son, J.; Park, S.H.; Kim, K.H.; et al. CT window trainable neural network for improving intracranial hemorrhage detection by combining multiple settings. *Artificial Intelligence in Medicine* **2020**, *106*, 101850.
114. Buls, N.; Watte, N.; Nieboer, K.; Ilsen, B.; de Mey, J. Performance of an artificial intelligence tool with real-time clinical workflow integration–detection of intracranial hemorrhage and pulmonary embolism. *Physica Medica* **2021**, *83*, 154–160.
115. Mushtaq, M.F.; Shahroz, M.; Aseere, A.M.; Shah, H.; Majeed, R.; Shehzad, D.; Samad, A. BHCNet: neural network-based brain hemorrhage classification using head CT scan. *Ieee Access* **2021**, *9*, 113901–113916.
116. Solorio-Ramírez, J.L.; Saldana-Perez, M.; Lytras, M.D.; Moreno-Ibarra, M.A.; Yáñez-Márquez, C. Brain hemorrhage classification in CT scan images using minimalist machine learning. *Diagnostics* **2021**, *11*, 1449.
117. Kim, K.H.; Koo, H.W.; Lee, B.J.; Yoon, S.W.; Sohn, M.J. Cerebral hemorrhage detection and localization with medical imaging for cerebrovascular disease diagnosis and treatment using explainable deep learning. *Journal of the Korean Physical Society* **2021**, *79*, 321–327.
118. Abe, D.; Inaji, M.; Hase, T.; Takahashi, S.; Sakai, R.; Ayabe, F.; Tanaka, Y.; Otomo, Y.; Maehara, T. A prehospital triage system to detect traumatic intracranial hemorrhage using machine learning algorithms. *JAMA Network Open* **2022**, *5*, e2216393–e2216393.
119. Hofmeijer, E.; Tan, C.; Van der Heijden, F.; Gupta, R. Crowd-sourced deep learning for intracranial hemorrhage identification: Wisdom of crowds or laissez-faire. *American Journal of Neuroradiology* **2023**, *44*, 762–767.
120. Lyu, J.; Xu, Z.; Sun, H.; Zhai, F.; Qu, X. Machine learning-based CT radiomics model to discriminate the primary and secondary intracranial hemorrhage. *Scientific Reports* **2023**, *13*, 3709.
121. Wang, R.; Li, C.; Wang, J.; Wei, X.; Li, Y.; Zhu, Y.; Zhang, S. Threshold segmentation algorithm for automatic extraction of cerebral vessels from brain magnetic resonance angiography images. *Journal of neuroscience methods* **2015**, *241*, 30–36.
122. Patel, A.; Schreuder, F.H.; Klijn, C.J.; Prokop, M.; Ginneken, B.v.; Marquering, H.A.; Roos, Y.B.; Baharoglu, M.I.; Meijer, F.J.; Manniesing, R. Intracerebral haemorrhage segmentation in non-contrast CT. *Scientific reports* **2019**, *9*, 17858.
123. Livne, M.; Rieger, J.; Aydin, O.U.; Taha, A.A.; Akay, E.M.; Kossen, T.; Sobesky, J.; Kelleher, J.D.; Hildebrand, K.; Frey, D.; et al. A U-Net deep learning framework for high performance vessel segmentation in patients with cerebrovascular disease. *Frontiers in neuroscience* **2019**, *13*, 97.
124. Wang, J.L.; Farooq, H.; Zhuang, H.; Ibrahim, A.K. Segmentation of intracranial hemorrhage using semi-supervised multi-task attention-based U-net. *Applied Sciences* **2020**, *10*, 3297.
125. Zhao, X.; Chen, K.; Wu, G.; Zhang, G.; Zhou, X.; Lv, C.; Wu, S.; Chen, Y.; Xie, G.; Yao, Z. Deep learning shows good reliability for automatic segmentation and volume measurement of brain hemorrhage, intraventricular extension, and peripheral edema. *European radiology* **2021**, *31*, 5012–5020.
126. Xu, J.; Zhang, R.; Zhou, Z.; Wu, C.; Gong, Q.; Zhang, H.; Wu, S.; Wu, G.; Deng, Y.; Xia, C.; et al. Deep network for the automatic segmentation and quantification of intracranial hemorrhage on CT. *Frontiers in neuroscience* **2021**, *14*, 541817.
127. Castro-Macías, F.M.; Morales-Álvarez, P.; Wu, Y.; Molina, R.; Katsaggelos, A.K. Hyperbolic Secant representation of the logistic function: Application to probabilistic Multiple Instance Learning for CT intracranial hemorrhage detection. *Artificial Intelligence* **2024**, *331*, 104115.
128. Xiao, H.; Shi, X.; Xia, Q.; Chen, L.; Chen, D.; Li, Y.; Li, L.; Liu, Q.; Zhao, H. DFMA-ICH: a deformable mixed-attention model for intracranial hemorrhage lesion segmentation based on deep supervision. *Neural Computing and Applications* **2024**, *36*, 8657–8679.
129. Zhang, L.; Miao, W.; Zhu, C.; Wang, Y.; Luo, Y.; Song, R.; Liu, L.; Yang, J. A weakly supervised-guided soft attention network for classification of intracranial hemorrhage. *IEEE Transactions on Cognitive and Developmental Systems* **2022**, *15*, 42–53.

 doi:10.20944/preprints202507.2393.v1

130. Kuo, W.; Hane, C.; Yuh, E.; Mukherjee, P.; Malik, J. Cost-sensitive active learning for intracranial hemorrhage detection. In Proceedings of the Medical Image Computing and Computer Assisted Intervention–MICCAI 2018: 21st International Conference, Granada, Spain, September 16-20, 2018, Proceedings, Part III 11. Springer, 2018, pp. 715–723.
131. Ginat, D. Implementation of machine learning software on the radiology worklist decreases scan view delay for the detection of intracranial hemorrhage on CT. *Brain Sciences* **2021**, *11*, 832.
132. Kyung, S.; Shin, K.; Jeong, H.; Kim, K.D.; Park, J.; Cho, K.; Lee, J.H.; Hong, G.; Kim, N. Improved performance and robustness of multi-task representation learning with consistency loss between pretexts for intracranial hemorrhage identification in head CT. *Medical Image Analysis* **2022**, *81*, 102489.
133. Sindhura, C.; Al Fahim, M.; Yalavarthy, P.K.; Gorthi, S. Fully automated sinogram-based deep learning model for detection and classification of intracranial hemorrhage. *Medical Physics* **2024**, *51*, 1944–1956.
134. Asif, M.; Shah, M.A.; Khattak, H.A.; Mussadiq, S.; Ahmed, E.; Nasr, E.A.; Rauf, H.T. Intracranial hemorrhage detection using parallel deep convolutional models and boosting mechanism. *Diagnostics* **2023**, *13*, 652.
135. Cortes-Ferre, L.; Gutierrez-Naranjo, M.A.; Egea-Guerrero, J.J.; Perez-Sanchez, S.; Balcerzyk, M. Deep learning applied to intracranial hemorrhage detection. *Journal of Imaging* **2023**, *9*, 37.
136. Jewel, S.; Robertas, A.; Bożena, F.; et al. Intracranial hemorrhage detection in 3D computed tomography images using a bi-directional long short-term memory network-based modified genetic algorithm. Journals. *Journals, Frontiers in neuroscience* **2023**, *17*.
137. Nie, T.; Chen, F.; Su, J.; Chen, G.; Gan, M. Knowledge-prompted intracranial hemorrhage segmentation on brain computed tomography. *Expert Systems with Applications* **2025**, p. 126609.
138. Nizarudeen, S.; Shanmughavel, G.R. Comparative analysis of ResNet, ResNet-SE, and attention-based RaNet for hemorrhage classification in CT images using deep learning. *Biomedical Signal Processing and Control* **2024**, *88*, 105672.
139. Tapia, G.; Allende-Cid, H.; Chabert, S.; Mery, D.; Salas, R. Benchmarking YOLO Models for Intracranial Hemorrhage Detection Using Varied CT Data Sources. *IEEE access* **2024**.
140. Emon, S.H.; Tseng, T.L.B.; Pokojovy, M.; Moen, S.; McCaffrey, P.; Walser, E.; Vo, A.; Rahman, M.F. Uncertainty-Guided Semi-Supervised (UGSS) mean teacher framework for brain hemorrhage segmentation and volume quantification. *Biomedical Signal Processing and Control* **2025**, *102*, 107386.
141. Park, A.; Chute, C.; Rajpurkar, P.; Lou, J.; Ball, R.L.; Shpanskaya, K.; Jabarkheel, R.; Kim, L.H.; McKenna, E.; Tseng, J.; et al. Deep learning–assisted diagnosis of cerebral aneurysms using the HeadXNet model. *JAMA network open* **2019**, *2*, e195600–e195600.
142. Cho, J.; Park, K.S.; Karki, M.; Lee, E.; Ko, S.; Kim, J.K.; Lee, D.; Choe, J.; Son, J.; Kim, M.; et al. Improving sensitivity on identification and delineation of intracranial hemorrhage lesion using cascaded deep learning models. *Journal of digital imaging* **2019**, *32*, 450–461.
143. Ye, H.; Gao, F.; Yin, Y.; Guo, D.; Zhao, P.; Lu, Y.; Wang, X.; Bai, J.; Cao, K.; Song, Q.; et al. Precise diagnosis of intracranial hemorrhage and subtypes using a three-dimensional joint convolutional and recurrent neural network. *European radiology* **2019**, *29*, 6191–6201.
144. Ker, J.; Singh, S.P.; Bai, Y.; Rao, J.; Lim, T.; Wang, L. Image thresholding improves 3-dimensional convolutional neural network diagnosis of different acute brain hemorrhages on computed tomography scans. *Sensors* **2019**, *19*, 2167.
145. Mansour, R.F.; Escorcia-Gutierrez, J.; Gamarra, M.; Diaz, V.G.; Gupta, D.; Kumar, S. Artificial intelligence with big data analytics-based brain intracranial hemorrhage e-diagnosis using CT images. *Neural Computing and Applications* **2023**, *35*, 16037–16049.
146. Anupama, C.; Sivaram, M.; Lydia, E.L.; Gupta, D.; Shankar, K. Synergic deep learning model–based automated detection and classification of brain intracranial hemorrhage images in wearable networks. *Personal and Ubiquitous Computing* **2022**, *26*, 1–10.
147. Sage, A.; Badura, P. Intracranial hemorrhage detection in head CT using double-branch convolutional neural network, support vector machine, and random forest. *Applied Sciences* **2020**, *10*, 7577.
148. Liu, Y.; Fang, Q.; Jiang, A.; Meng, Q.; Pang, G.; Deng, X. Texture analysis based on U-Net neural network for intracranial hemorrhage identification predicts early enlargement. *Computer Methods and Programs in Biomedicine* **2021**, *206*, 106140.
149. Mansour, R.F.; Aljehane, N.O. An optimal segmentation with deep learning based inception network model for intracranial hemorrhage diagnosis. *Neural Computing and Applications* **2021**, *33*, 13831–13843.

 doi:10.20944/preprints202507.2393.v1

150. Zhang, G.; Chen, K.; Xu, S.; Cho, P.C.; Nan, Y.; Zhou, X.; Lv, C.; Li, C.; Xie, G. Lesion synthesis to improve intracranial hemorrhage detection and classification for CT images. *Computerized Medical Imaging and Graphics* **2021**, *90*, 101929.
151. Angkurawaranon, S.; Sanorsieng, N.; Unsrisong, K.; Inkeaw, P.; Sripan, P.; Khumrin, P.; Angkurawaranon, C.; Vaniyapong, T.; Chitapanarux, I. A comparison of performance between a deep learning model with residents for localization and classification of intracranial hemorrhage. *Scientific Reports* **2023**, *13*, 9975.
152. Fan, J.; Fan, X.; Song, C.; Wang, X.; Feng, B.; Li, L.; Lu, G. Dual-task vision transformer for rapid and accurate intracerebral hemorrhage CT image classification. *Scientific Reports* **2024**, *14*, 28920.
153. Ramananda, S.H.; Sundaresan, V. Label-efficient sequential model-based weakly supervised intracranial hemorrhage segmentation in low-data non-contrast CT imaging. *Medical Physics* **2025**, *52*, 2123–2144.